Available to the public.

TECHNICAL INFORMATION SERIES

R67SD57

APPLICATION OF FIBROUS COMPOSITE MATERIALS TO LARGE ROCKET SYSTEMS

B. W. ROSEN,
R. SNYDER,
N. F. DOW

SPACE SCIENCES LABORATORY

MISSILE AND SPACE DIVISION

GENERAL ELECTRIC

SPACE SCIENCES LABORATORY

MECHANICS SECTION

APPLICATION OF FIBROUS COMPOSITE MATERIALS TO LARGE ROCKET SYSTEMS

By

B. Walter Rosen
Roger Snyder
N. F. Dow

Prepared for the National Aeronautics and Space Administration
under Contract NAS2-3811

October 1967
R67SD57

MISSILE AND SPACE DIVISION

GENERAL ELECTRIC

ABSTRACT

Studies of the potential for minimization of structural weight in large launch vehicles of the future through the use of composite materials are described. Previous structural weight minimization techniques for composites are reviewed and extended. Typical structural efficiency charts are presented. Significant weight saving through the application of an efficiently stiffened composite structure is demonstrated.

ACKNOWLEDGEMENT

The work on this study was performed by the General Electric Company for the National Aeronautics and Space Administration under Contract NAS2-3811, monitored by Mr. E. Gomersall and Mr. K. Nishioka of the Mission Analysis Division of the Office of Advanced Research and Technology. The work described herein was conducted at the Space Sciences Laboratory as a part of the program conducted at the Apollo Support Department. The cooperation of the members of the Program Support Group at ASD is acknowledged.

CONTENTS

INTRODUCTION

An area of substantial promise for the increase in launch vehicle payload capacity is the use of advanced materials in the primary structure. Previous work (Ref. 1) has indicated the efficiency of filament wound composites for cylinders under axial compression. Recent advances in strength and stiffness of filamentary materials have enhanced the potential for filament wound composite pressure vessels. Therefore, a quantitative analysis has been performed to assess the weight savings made possible by the use of composites, containing glass, boron and carbon filaments, as the primary structure of launch vehicles.

Attention was directed toward the million-pound-to-orbit class boost vehicles. These studies evaluate minimum structural weight of stiffened shells as a function of the design load and overall structural geometry. Specific designs are obtained for general post-Saturn-class launch vehicles. Results are compared with similar designs for metallic structures obtained in Reference 2. The principal result of the studies is the demonstration of substantial potential in terms of boost vehicle structural weight reduction for advanced fibrous composite shells utilizing efficient stiffening.

SCOPE OF THE ANALYSIS

Design Requirements

The major advances to be accomplished through the use of composite materials will require materials presently in the early stages of development. Therefore, it is appropriate to examine these advanced materials on vehicles which have yet to be built. The launch vehicles selected are in the million-pound-to-orbit class and include both single- and two-stage-to orbit vehicles. These vehicles have been examined in Reference 2 for a variety of materials and design criteria. The present paper utilizes several of the overall configurations of Reference 2 as shown in Figures 1-3.

Load envelopes, shown in Figures 4-6, were also taken from Reference 2. These design loads were determined by calculating the rigid body response to inflight wind loads and pre-launch wind conditions. This response was then used to calculate the distribution of axial forces and bending moments along the vehicle's axis. Finally these axial forces and bending moments were combined with propellant tank pressures and were resolved into stress resultants in the plane of the shells which comprise the vehicle's structure. The following critical loading conditions were considered:

1. Pre-launch - Unpressurized tanks with 99.9% wind conditions.
2. Pre-launch - Pressurized tanks with 99.9% wind conditions.
3. Maximum $q\alpha$ in flight (q is dynamic pressure and α is angle of attack).
4. Maximum acceleration in flight

Typical force, moment and shear distribution curves and pressure history curves are shown in Figures 4-5. Figure 6 indicates a typical maximum stress resultant distribution. Similar results are given for the remaining configurations in Reference 2.

Design weights for the three vehicles of Figures 1-3 were obtained in Reference 2 for a vehicle of "nominal" construction, primarily an efficiently stiffened aluminum alloy structure. The weights of these "nominal" vehicles are shown in Table I. Design weights obtained in this report are compared with the weights of these "nominal" vehicles.

The vehicle structure was divided into two categories. The first included all external structure, vehicle skin and major tank heads. Composite materials were considered for these structural elements. The second category included other structural weights, such as baffles, hung tanks, thrust structure, etc. These weights were held fixed at the values reported in Reference 2 and shown in Table I.

The analytical methods used have drawn extensively on the structural efficiency methods developed in Reference 1 and applied in Reference 3. These studies evaluate minimum structural weight as a function of the design load and the structural geometry. These latter factors are defined by the structural index. The structural design of the advanced configurations treated in this report is governed by values of the structural index which lie within the range covered by contemporary boost vehicles (see Ref. 3). Thus, the general conclusions of the previous studies are applicable to the presently considered vehicles. These conclusions will be reviewed subsequent-

ly. Failure criteria for pressurized tanks, in those regions where the circumferential tension in the tank wall was combined with axial compression, involved significant departures from previous methods. These will be discussed further in subsequent sections. Selection of appropriate materials and structural configurations drew on the previous experience with smaller vehicles.

Materials Selection

The composites chosen for consideration in this program are: A high-modulus glass fiber in an epoxy binder, a representative, present-day material that has already been used for similar applications; a boron fiber/epoxy composite which represents the stiffest continuous fiber available and a matrix which can be readily fabricated into composite form; and finally, a carbon filament/aluminum matrix, which represents an advanced composite now available in laboratory form. These materials were chosen to represent the spectrum of properties, readily foreseeable for future use. Properties of the above constituents are present in Table II. The composites formed by arranging a parallel set of fibers in the matrix (a "uniaxial" composite) are transversely isotropic and have five independent elastic moduli. These are evaluated by the methods of Reference 4. The average of the "upper" and "lower" bounds of that reference are used and the results are presented in Table III. These are the properties of the individual lamina used to construct the various laminates studied during this program. The strengths of these laminae are also presented in Table III. Shear and transverse com-

posite strengths were assumed to be equal to the matrix strengths (see Ref. 12). Longitudinal tensile strengths were based on experimental data and longitudinal compressive strengths were computed by the methods of Reference 5.

Additionally, an evaluation of future potential should assess whiskers and other high modulus filaments. A recent study (Ref. 6) has shown that properly designed discontinuous fiber composites can be expected to have essentially the same properties as continuous fiber composites of the same constituents. For the present compressive application, the important properties are the elastic stiffnesses and the compressive strengths. These properties are governed primarily by fiber modulus, binder modulus and binder yield strength (Ref. 4 and 5). Since the boron and carbon fibers are very close in stiffness to other available high modulus fibers and whiskers, the results for boron/epoxy and carbon/aluminum composites can be considered representative of other composites having the given matrix material.

Another area of potential improvement is associated with the use of shaped fibers designed to improve the transverse properties of a uniaxial composite. The National Research Corporation has developed a process for the deposition of thin films of boron on a plastic substrate (Ref. 7). The important characteristic of these thin films is that they have demonstrated the same high mechanical properties as boron filaments. Thus by cementing together layers of these films one can build up a laminated composite

having biaxial properties approaching those of the primarily uni-directional properties of the filamentary composites. At present, the thickness of the plastic substrate used limits the volume fraction of boron in the laminated films to 30%. This material has a modulus which is slightly higher and a density slightly lower than those of the isotropic boron/epoxy composite and will differ little in performance from the latter material. However, Reference 7 projects ahead to 50% volume fraction boron; and it is possible that the performance of such a composite (yet to be evaluated) would be substantially superior to that for other boron/epoxy composites considered.

Configuration Selection

Two principal structural configurations were selected for the cylindrical and conical shell sections of the vehicles under consideration. As a reference point, monocoque composite shells were evaluated. These laminates were considered to have laminae each containing a uni-directional set of fibers. Directions of principal stiffness of the laminae were varied symmetrically such that the directions of principal stiffness of the laminate were coincident with the axial and circumferential directions. Further, patterns were selected so that coupling effects were minimized and could be neglected.

The second structural configuration is the honeycomb core sandwich shell. This was selected to represent the general case of efficient stiffening. Here the core was assumed to have adequate stiffness to stabilize the face sheets so that the sandwich failed due to overall instability. The core

was assumed to carry no load. The face sheets had the properties described for the monocoque shells.

Two laminate patterns were selected for this study based on the results of References 1 and 8. These were a pseudo-isotropic pattern ($\pm 60^{\circ}$, 0°) and a 0°-90° pattern. The previous studies (Ref. 8) have indicated that this "isotropic" pattern is most efficient when stability is the governing design criterion. This is indicated in Figure 7 where the structural weight parameter, $f = (W/R)/(N_x/R)^{1/2}$ of glass/epoxy is plotted for various laminate patterns. This parameter is valid over the range of index values for which the shell failure mode is elastic instability. It can be seen that the isotropic shell is significantly lighter than all symmetric biaxial ($\pm\theta$) laminates and all orthogonal (0°-90°) laminates. However the isotropic laminates do not fully utilize the load carrying capabilities of uniaxial composites. For the high axial loads, for which strength is the governing criterion, a 0°-90° laminate (with most fibers in the direction of the load) will be more efficient. Table IV presents the structural weight parameter for stability and the axial yield strength (in compression) of various 0°-90° laminates, and, for comparison purposes, of the "isotropic" laminates.

Three 0°-90° patterns were selected on the basis of the results shown in Table IV in order to have high strength materials for comparative evaluation. For the glass/epoxy laminate, 85% of the fibers in the 0° direction was selected as the maximum amount representative of current fabrication capability. For the boron/epoxy laminate, 95% of the fibers in the 0° direc-

tion were used as representative of future possibilities. Since the carbon-aluminum laminate is relatively insensitive to changes in the percent of axial fibers present, it was decided to use a more easily achievable value of 90% for the purposes of this study.

Isotropic laminates were found to be most efficient in regions where axial thrust was combined with pressure loading. A separate study of six 0°-90° boron/epoxy laminates was made for these regions (see Table V). The amount of material in the 0° layer was taken as $\frac{1}{4}$, $\frac{1}{3}$, $\frac{2}{5}$, $\frac{1}{2}$, $\frac{3}{5}$, and $\frac{2}{3}$ of the total thickness. Some of the properties of these laminates can be compared to the values for the boron/epoxy "isotropic" laminates given in Table IV.

Boron/epoxy was selected because this combination shows the greatest variation in strengths (see Table IV). Although the carbon/aluminum or glass/epoxy 0°-90° laminate is more likely to be more efficient than the "isotropic" laminate, the difference in final weights is insignificant because of the small variations in the strengths of these composites.

The results of the above study showed that only in the case of the lightest-cored sandwich shell applied to the heaviest loaded section of tank, was a 0°-90° laminate more efficient. Since, at other sections of the same tank, the study showed that an "isotropic" laminate was more efficient, and since it is not feasible to fabricate a single tank with two types of windings, it was decided to use "isotropic" laminates for all pressurized fuel tanks. $\pm 45^{\circ}$ (orthogonal) laminates were selected for the tank heads, since they

were subjected to pressure loadings only. The relative thicknesses of the two layers were determined by the relative sizes of the meridional and circumferential membrane forces.

METHODS OF ANALYSIS

The structural efficiency analysis used involves the determination of generalized weights of structural shell required to carry given axial loading intensities. The appropriate parameters for this generalization have been found to be (e. g. Ref. 1) weight per unit surface area divided by shell radius (W/R), as a function of axial load per unit length of circumference divided by shell radius (N_x/R). Evaluations of the minimum-weight configuration in each case required the application of the appropriate shell failure criteria, which were taken here as either elastic buckling or compressive yielding or fracture. Circumferential loads due to pressure in thrust carrying shells were included in the strength criterion but conservatively neglected in the stability criterion.

Stability Criterion

The elastic buckling criterion is based on the small-deflection orthotropic shell stability results of Reference 1, wherein it is shown that the buckling mode is governed by a parameter Φ; where $\Phi = (\gamma)^{1/2}$ or 1, whichever is smaller. The shear stiffness ratio γ is given by

$$\gamma = \frac{2G_{LT}\left[1+(\nu_{LT}\nu_{TL})^{1/2}\right]}{(E_L E_T)^{1/2}}$$

where G_{LT} is the shear modulus in the plane of the shell, E_L and E_T are the longitudinal (axial) and transverse (circumferential) stretching moduli

of the shell, and ν_{LT} and ν_{TL} are the Poisson's ratios.

If $\gamma > 1$, the buckling mode is symmetric (Bellows-type deformation) and the buckling stress σ_{CR} is given by

$$\sigma_{CR} = \frac{k}{\sqrt{3}} \frac{t}{R} \overline{E}$$

where $\overline{E}$ is the effective stiffness given by

$$\overline{E} = \left[\frac{E_L E_T}{(1-\nu_{LT}\nu_{TL})}\right]^{1/2}$$

and t is the shell thickness, R is the shell radius, and k is the empirical knockdown factor ($k \leq 1$). If $\gamma < 1$, the buckling mode is asymmetric (checkerboard type deformations)and

$$\sigma_{CR} = \frac{k}{\sqrt{3}} \left(\frac{t}{R}\right) \left[\frac{2 G_{LT} (E_L E_T)^{1/2}}{1 - (\nu_{LT}\nu_{TL})^{1/2}}\right]^{1/2}$$

The structural efficiency equation employing this expression for elastic buckling is

$$\frac{W}{R} = \frac{\rho_S \left[\frac{N_x}{R}\right]^{1/2}}{\left[\frac{k}{\sqrt{3}} \overline{E} \Phi\right]^{1/2}}$$

where, as before, Φ is $(\gamma)^{1/2}$ or 1, whichever is smaller, and N_x is the axial load divided by the shell circumference. This procedure is applicable only to simple monocoque shells, but illustrates the methods used through-

out this study. Details of the application of these methods to sandwich shells are presented in Reference 1.

Strength Criterion

When a laminate is subjected to a known set of stress resultants, the average stresses in any lamina can be computed by the Space Sciences Laboratory LILAC program (Ref. 9). With a strength criterion defined for a single lamina, it is possible to construct an approximation to the laminate stress-strain curve.

The strength criterion which was utilized for the individual lamina is a maximum stress criterion based on the extensional strengths in the longitudinal and transverse directions and the in-plane shear strength with respect to the principal elastic axes. These strengths (listed in Table III) are based on: experimental data for the longitudinal tensile stress; on methods discussed in Reference 5 for the longitudinal compressive strength; and on those in Reference 12 for in-plane shear and transverse direct stress.

Two cases of failure are considered. Whenever a stress component in the fiber direction (σ_1) equal the assumed longitudinal strength of the particular layer, immediate laminate failure is postulated. In the second case, when the transverse normal stress or in-plane shear stress reaches the maximum allowable value, it is postulated that that particular stress component remains constant and that the transverse Young's modulus (E_2) and in-plane shear modulus (G_{12}) drop to zero in that layer. This procedure yields a piecewise linear stress-strain curve leading to a horizontal slope

or ultimate stress condition.

For the present report, the lowest maximum lamina stress condition was evaluated and defined as the laminate material yield stress. Then E_2 and G_{12} was set to zero in every layer, leaving only the extensional stiffness in the fiber direction (E_1) as a non-zero quantity. Using this "netting" analysis procedure, the lowest average stress which led to a lamina failure (in the fiber direction) was defined as the material ultimate stress.

Typical stress-strain curves (for uniaxial loading) derived by the above method are shown in Figure 8. The simplified procedure bypasses the need for analytic determination of the entire stress-strain curve. Rather, the initial departure from elastic behavior is evaluated and the maximum stress is conservatively estimated. Hence, the procedure is suitable for parametric studies such as the present one.

The failure mode at the yield limit depends upon the relationship between the load vector and fiber orientation. This is illustrated by Figure 9 for a symmetric bi-axial ($\pm\theta$ fiber orientation) composite subjected to axial tension ($\theta = 0^{o}$). The relative importance of the various failure modes depends upon the relative stiffnesses of the fiber and matrix materials. For example, in Figure 10, where interaction curves for isotropic laminates are plotted, it is seen that for certain load vectors a carbon/aluminum isotropic laminate may be weaker than a boron/epoxy isotropic laminate, although the individual lamina are stronger. The stress distributions in the type of laminates considered in this study are shown in Table VI.

Design Methods

The minimum thickness required to prevent a strength failure was taken as the thickness which will resist 1.1 times the load at yield and 1.4 times this load at ultimate. For combined loads (axial and transverse loads) the required thickness for the "isotropic" laminates can be found from Figure 10. This graph was constructed using the previously described strength criteria. The 1.1 and 1.4 factors were included. Values of N_x/t for the 0° -90° laminates considered (for axial load only) can be found in Table VII.

The monocoque shells subjected to additional axial load were sized to have at least this required minimum thickness and to resist stability failure under 1.4 times the maximum axial load to which they were subject. Thus the stability criterion was on the conservative side since the internal pressure was neglected.

For a sandwich shell, an optimum core thickness to face sheet thickness was determined, (Ref. 1). Then the total face sheet thickness, for a sandwich with this ratio of thicknesses, necessary to resist a stability failure at 1.4 times the maximum axial load was determined. If this face sheet thickness was less than that necessary to resist 1.1 times the total load (including pressure) at yield and 1.4 times this load at ultimate, then the face sheet thickness necessary to resist this strength failure was used. The core thickness was adjusted to prevent stability failure. In this case, the ratio of the two thicknesses is no longer optimum.

Besides the 1.1 yield factor of safety and the 1.4 ultimate factor of safety, several others were included into the design. An empirical knockdown factor, k, taken from Reference 10, was included in the stability studies. In these computations, elastic stiffnesses were used for simplicity. In actuality when ultimate stress governs the face sheet thickness of the sandwich shell, a reduced modulus would be appropriate. Neglect of this reduces the buckling margin in these cases to an unassessed value which is less than 40%. However, at 1.1 times the design load, the skins will be stressed elastically, since, in these cases, the skin thickness for the ultimate stress criterion is greater than that for the yield stress criterion. Also, the core thickness was selected to assure elastic stability under a load equal to 1.4 times the design load. Thus, it is clear that at 1.1 times the load, the design is elastic and stable; hence, the buckling margin is in excess of 10%. A fabrication factor of 1.05 for monocoque and 1.25 for sandwich shells was also included in all calculations. For those cases in which a pressurized tank was to be subjected to cryogenic temperatures, a two mil aluminum liner was included in the tank weight.

RESULTS

Material Characteristics

The strength characteristics of the selected 0°-90° laminates, subjected to axial compression, are given in Table VII. The appropriate safety factors have been included. Failure is due to the stress transverse to the fibers in the 90° layer. Similar characteristics are presented for the isotropic laminate in Figure 10. The graph includes values for combined loads of internal pressure and axial compression or tension. The modes of failure at a series of points on the graph is given in Table VIII. Note that when the two load resultants are of opposite sign the relative ranking of the boron/epoxy and the carbon/aluminum materials varies with the ratio of these resultants. The different failure modes for the laminates account for the discontinuities in the curves. The stress distributions upon which these curves are based can be seen in Table VI.

Plots of the efficiency curves (W/R) vs (N_x/R) are given in Figure 11-13 for all three materials and both structural configurations. These graphs include both the stability and strength criteria. In addition, the empirical knockdown factor and fabrication factors are also included. Both the 0°-90° and "isotropic" laminates are shown. Some general observations can be made from these graphs for the range of (N_x/R) of interest. It can be seen that sandwich shells, as expected, are more efficient than the monocoque design.

"Isotropic" laminates are generally more efficient than 0°-90° laminates. Only for those high structural index values and for efficient stiffening (i.e. low core density) where a strength criterion governs the face sheet thickness does the 0°-90° laminate become more efficient, and then only if the value of f (see Table IV) for this laminate is close to that for the "isotropic" case. The 0°-90° laminate would be more efficient for the monocoque shell only if the strength criterion governed, which does not occur for the values of (N_x/R) of interest.

Finally, it should be noted that the differences between the 0°-90° laminate and the "isotropic" laminate is greatest for boron/epoxy and least for carbon/aluminum. This is due to the fact that the ratio of the stiffnesses of fiber and matrix material is greatest for boron/epoxy and least for carbon/aluminum.

The effect of the strength criterion on the efficiency curves is illustrated in Figures 14-16. In these graphs the stability criterion is applied to the maximum axial load, whereas the strength criterion is applied to the combined axial load and internal pressure. Curves for axial compression acting alone are re-plotted (as the solid lines) from Figures 11-13 for comparison purposes.

In general, carbon/aluminum represents the most efficient "isotropic" laminate and glass/epoxy the least efficient of the three studied. However, in regions where strength becomes the governing criterion (particularly for light-cored sandwich shells) and for load combinations where the strength

of boron/epoxy is greater than that of carbon/aluminum (see Figure 10); boron/epoxy becomes the more efficient laminate. The efficiency curves for the monocoque shells do not depend upon the load combination because these curves are governed by the stability criterion for the range of (N_x/R) considered.

Total Weights

Weights for the three vehicle configurations considered (Figs. 1-3) are shown in Tables IX-XI. These weights include fixed weights (Table I), monocoque tank heads, and pressurized and unpressurized shell sections. The weights are tabulated by material and structural configuration. Finally, the total weights are given and percentage comparisons with the "nominal" vehicle (Table I) tabulated.

The figures showing the percent weight savings over the "nominal" vehicle weights are summarized in Figure 17. In general, only with a carbon/aluminum composite can the monocoque construction match the efficiently stiffened aluminum structure of the "nominal" vehicle construction. However, if efficient stiffening is also included with the use of composite materials (as represented by light-cored sandwich shells) as much as 60% of the nominal weight can be saved.

Note that the 301 vehicle configuration shows the widest variation in weight. Also, for this vehicle, the light-cored sandwich (ρ_C = .001 pci) boron/epoxy structure is slightly more efficient than the corresponding carbon/aluminum structure. Both of these facts can be attributed to the

percentage of structural weight in the LH_2 tank cylinder which is an integral part of the thrust-carrying structure.

Another observation is that the more efficient the stiffening, the less variation in weight savings from vehicle to vehicle for a given material. This is due to two reasons. First, for the lighter constructions, the total weight of the particular vehicle is closer to the fixed weights of the tank supports, thrust structure, insulation, etc. Second, for efficient stiffening, the vehicle is close to failure by both the stability criterion and the strength criterion, making the maximum use of the given material. The more efficient the stiffening, the smaller the added core weight necessary to achieve stability.

For purposes of comparison, Figure 18 presents some of the results obtained in Reference 2. Shown are the results of combining the use of Titanium or Beryllium with an efficient stiffening system. In all cases, with the exception of Beryllium construction of the 101 configuration, that stiffening system was honeycomb sandwich. In the one exception single face corrugation proved to be more efficient (see Ref. 2). Also shown are the results obtained if all structural weight is reduced to zero with the exception of the fixed weights.

CONCLUSIONS

The conclusions from this phase of the study are the following:

1. Fibrous composites using high modulus, high strength filaments offer the potential for substantial reductions with respect to conventional metallic design in boost vehicle structural weight. However, similar weight reductions are also indicated for efficiently stiffened Beryllium structures.

2. Achievement of these weight savings requires the use of efficient shell stiffening configurations such as low core density sandwiches, for interstage structures, and high tensile strength for tank structures.

Additionally, it is of value to restate, with some modifications, certain of the conclusions of the earlier study (Ref. 3) of contemporary boost vehicles of composite design, namely:

3. For the significant range of loading index over which optimum designs for compression shells fail by elastic instability, high modulus, filaments in an isotropic laminate are lighter than metal shells. Indeed, relatively small volume concentrations of such filaments produce materials of comparable efficiency to metals.

4. For sandwich construction, the elastic shell buckling efficiency is no longer proportional to the ratio of shell density, ρ_s, and to the square root of Young's modulus, E_s, as for a monocoque shell, but rather is proportional to $(\rho_s/E_s)^{1/2}$ for the sandwich face material.

5. Poor lamina in-plane shear strength and transverse extensional strength result in poor strength performance of laminates. Configurations which are considerably heavier than optimum for buckling must frequently be used to satisfy strength requirements. Effort to achieve improvement in matrix properties is indicated.

REFERENCES

1. Dow, N. F. and Rosen, B. W., "Structural Efficiency of Orthotropic Shells Subjected to Axial Compression," AIAA Journal, Vol. 4, No. 3, pp. 481-485, March 1966.

2. _____, "Study of Structural Weight Sensitivities for Large Rocket Systems, Final Report," Apollo Support Department, Missile and Space Division, General Electric Company (prepared under NASA Contract NAS2-3811), 7 July 1967.

3. Rosen, B. W. and Dow, N. F., "Influence of Constituent Properties upon the Structural Efficiency of Fibrous Composite Shells," J. of Spacecraft and Rockets, Vol. 3, No. 9, pp. 1377-1384, September 1966.

4. Hashin, Z. and Rosen, B. W., "The Elastic Moduli of Fiber Reinforced Materials," J. of Applied Mechanics, Series E, Vol. 31, No. 2, 1964.

5. Rosen, B. W., "Mechanics of Composite Strengthening," Fiber Composite Materials, ASM, Metals Park, Ohio, 1965.

6. Friedman, E., "A Tensile Failure Mechanism for Whisker Reinforced Composites," Paper No. 4A, presented at the 22nd Annual SPI Reinforced Plastics Division Conference, Washington, D. C., January 1967.

7. _____, "Advanced Filaments and Composites Program Review," WPAFB, December 6-8, 1965.

8. Dow, N. F., Rosen, B. W. and Hashin, Z., "Studies of Mechanics of Filamentary Composites," NASA CR-492, June 1966.

9. Rosen, B. W., "Elastic Analysis of Fibrous Composites and Non-Homogeneous Laminates," Mechanics Section Report No. 66-101, Space Sciences Laboratory, Missile and Space Division, General Electric Co., June 1966.

10. _____, "Buckling of Thin-Walled Circular Cylinders," NASA SP-8007, pp. 13 and 37, September 1965.

11. _____, "Study of the Relationship of Properties of Composite Materials to Properties of Their Constituents, "Quarterly Progress Report No. 3, NASw-1377, February 1967, to be published.

12. Shu, L. and Rosen, B. W., "Application of the Methods of Limit Analysis to the Evaluation of the Strength of Fiber-Reinforced Composites," to be published.

TABLE I

NOMINAL WEIGHTS

101 CONFIGURATION

Section	Weight Lb.
Instrument Unit	8736
Forward Skirt	12523
LH_2 Tank Top Head	10557
LH_2 Tank Cylinder	24613
LH_2 Tank Bottom Head	12464
Intertank	35527
Baffles & Insulation	23740
LOX Tank & Thrust Str.	54546
Aft. Skirt	121428
2nd Stage Total	304134
Interstage	33583
Forward Skirt	52357
LOX Tank Top Head	8345
LOX Tank Cylinder	20971
LOX Tank Bottom Head	14614
Intertank	135205
RP-1 Tank Top Head	8075
RP-1 Tank Bottom Head	10923
Thrust Takeout	47291
Thrust Structure	81537
Baffles & Insulation	39270
1st Stage Total	452171
Total Weight	756305

201 CONFIGURATION

Section	Weight Lb.
IU & Forward Skt.	13004
LH_2 Tank & Thrust Str.	39323
Intertank	38963
Baffles & Insulation	12900
LOX Tank	8850
Aft. Skirt	10389
2nd Stage Total	123429
Interstage	65266
Forward Skirt	46882
LOX Tank Top Head	8746
LOX Tank Bottom Head	19318
Intertank	156026
LH_2 Tank Top Head	15935
LH_2 Tank Cylinder	63411
LH_2 Tank Bottom Head	35330
Thrust Takeout	53698
Thrust Structure	82741
Baffles & Insulation	20040
1st Stage Total	567393
Total Weight	690822

301 CONFIGURATION

Section	Weight Lb.
Instrument Unit	13647
Forward Skirt	52748
LOX Tank Top Head	14489
LOX Tank Cylinder	5189
Common Bulkhead	63425
LH_2 Tank Cylinder	316615
LH_2 Tank Bottom Head	22287
Thrust Takeout	78745
Thrust Structure	56175
Insulation	18000
Total Weight	641320

TABLE II

PROPERTIES OF CONSTITUENT MATERIALS

Fiber	E, psi	ν	ρ, pci
Glass	16.0×10^6	0.20	0.0914
Boron	60.0×10^6	0.20	0.0830
Carbon	60.0×10^6	0.18	0.0720

Binder	E, psi	ν	ρ, pci
Epoxy	0.5×10^6	0.35	0.050
Aluminum	10.7×10^6	0.32	0.100

TABLE III

PROPERTIES OF UNIAXIAL FIBROUS COMPOSITES

(30% Binder Volume)

Composite	E_L, psi	E_T, psi	G_{LT}, psi	G_{TN}, psi	ν_{TL}
Glass/Epoxy	11.4×10^6	2.5×10^6	0.91×10^6	0.93×10^6	0.238
Boron/Epoxy	42.1×10^6	2.9×10^6	1.0×10^6	1.0×10^6	0.237
Carbon/Aluminum	45.3×10^6	31.2×10^6	12.4×10^6	12.1×10^6	0.216

Composite	ρ, pci	Tension $(\sigma_y)_L$, psi	Compression $(\sigma_y)_L$, psi	$(\sigma_y)_T$, psi	$(\tau_y)_{LT}$, psi
Glass/Epoxy	0.0790	2×10^5	1.13×10^5	$.1 \times 10^5$	$.1 \times 10^5$
Boron/Epoxy	0.0731	2×10^5	4.21×10^5	$.1 \times 10^5$	$.1 \times 10^5$
Carbon/Aluminum	0.0804	2×10^5	4.53×10^5	$.7 \times 10^5$	$.35 \times 10^5$

TABLE IV

PROPERTIES OF 0°-90° AND "ISOTROPIC" LAMINATES

Laminate Configuration	Glass/Epoxy		Boron/Epoxy		Carbon/Aluminum	
	σ_y, psi	f, $(lb)^{1/2}/(ft)^2$	σ_y, psi	f, $(lb)^{1/2}/(ft)^2$	σ_y, psi	f, $(lb)^{1/2}/(ft)^2$
0°-.7t	35.1×10^3	0.00781	107×10^3	0.00538	93.5×10^3	0.00262
0°-.75t	36.9×10^3	0.00784	114×10^3	0.00543	95.0×10^3	0.00262
0°-.8t	38.7×10^3	0.00789	121×10^3	0.00550	96.5×10^3	0.00262
0°-.85t	40.6×10^3	0.00795	128×10^3	0.00560	98.2×10^3	0.00262
0°-.9t	42.7×10^3	0.00802	136×10^3	0.00574	100×10^3	0.00262
0°-.95t	44.6×10^3	0.00811	144×10^3	0.00594	102×10^3	0.00262
0°-t	$46.9 \times 10^{3*}$	0.00822	$155 \times 10^{3*}$	0.00628	$103 \times 10^{3*}$	0.00262
Isotropic	37.8×10^3	0.00632	81.4×10^3	0.00339	93.0×10^3	0.00252

* Limiting Value as $t_{90^o} \rightarrow 0$ (see Table III)

For Monocoque Shells $\frac{W}{R} = f \left(\frac{N_X}{R}\right)^{1/2}$

σ_y = yield stress in compression

TABLE V

PROPERTIES OF 0°-90° BORON/EPOXY LAMINATES

LAMINATE	f, $(lb)^{1/2}/(ft)^2$	(σ_y), psi
$\frac{2}{3} \rightarrow 0^{\circ}$	.00535	102×10^3
$\frac{3}{5} \rightarrow 0^{\circ}$	.00531	91.8×10^3
$\frac{1}{2} \rightarrow 0^{\circ}$	.00529	78.7×10^3
$\frac{2}{5} \rightarrow 0^{\circ}$	.00531	65.0×10^3
$\frac{1}{3} \rightarrow 0^{\circ}$	.00535	55.9×10^3
$\frac{1}{4} \rightarrow 0^{\circ}$	.00543	44.3×10^3

TABLE VI

STRESS DISTRIBUTIONS IN LAMINATES

LAMINATE	$N_x = 1.0$, $N_y = 0.0$			$N_x = 0.0$, $N_y = 1.0$		
	σ_1	σ_2	σ_{12}	σ_1	σ_2	σ_{12}
Glass/Epoxy						
$\frac{1}{3}t \rightarrow +60^\circ$	0.132	0.327	-0.191	1.452	0.009	0.191
$\frac{1}{3}t \rightarrow 0^\circ$	2.113	-0.029	0.0	-0.528	0.445	0.0
$\frac{1}{3}t \rightarrow -60^\circ$	0.132	0.327	0.191	1.452	0.089	-0.191
Boron/Epoxy						
$\frac{1}{3}t \rightarrow +60^\circ$	0.054	0.123	-0.073	1.790	0.031	0.073
$\frac{1}{3}t \rightarrow 0^\circ$	2.660	-0.015	0.0	-0.816	0.169	0.0
$\frac{1}{3}t \rightarrow -60^\circ$	0.054	0.123	0.073	1.790	0.031	-0.073
Carbon/Aluminum						
$\frac{1}{3}t \rightarrow +60^\circ$	0.231	0.642	-0.375	0.926	0.201	0.375
$\frac{1}{3}t \rightarrow 0^\circ$	1.271	-0.019	0.0	-0.116	0.862	0.0
$\frac{1}{3}t \rightarrow -60^\circ$	0.231	0.642	0.375	0.926	0.201	-0.375
Glass/Epoxy						
$.85t \rightarrow 0^\circ$	1.133	.021	0.0	-0.021	0.654	0.0
$.15t \rightarrow 90^\circ$	-0.118	0.246	0.0	2.961	0.118	0.0
Boron/Epoxy						
$.95t \rightarrow 0^\circ$	1.049	0.007	0.0	-0.007	0.593	0.0
$.05t \rightarrow 90^\circ$	-0.131	0.069	0.0	8.732	0.131	0.0
Carbon/Aluminum						
$.90t \rightarrow 0^\circ$	1.033	0.007	0.0	-0.007	0.955	0.0
$.10t \rightarrow 90^\circ$	-0.062	0.701	0.0	1.402	0.062	0.0

TABLE VII

STRENGTH OF 0°-90° LAMINATES

Glass/Epoxy $(0^{\circ}-.85t,\ 90^{\circ}-.15t)$

$\frac{N_x}{t} = 36.9 \times 10^3$ psi

Boron/Epoxy $(0^{\circ}-.95t,\ 90^{\circ}-.05t)$

$\frac{N_x}{t} = 131.0 \times 10^3$ psi

Carbon/Aluminum $(0^{\circ}-.90t,\ 90^{\circ}-.10t)$

$\frac{N_x}{t} = 91 \times 10^3$ psi

TABLE VIII

MODES OF FAILURE OF ISOTROPIC LAMINATES

$M^{(4)}$	Glass/Epoxy			Boron/Epoxy			Carbon/Aluminum		
	$Y/U^{(1)}$	$Layer^{(2)}$	$\sigma^{(3)}$	$Y/U^{(1)}$	$Layer^{(2)}$	$\sigma^{(3)}$	$Y/U^{(1)}$	$Layer^{(2)}$	$\sigma^{(3)}$
0	Y	$\pm 60^{\circ}$	σ_2	U	0°	σ_1^+	U	0°	σ_1^+
1	Y	$\pm 60^{\circ}$	σ_2	U	0°	σ_1^+	U	0°	σ_1^+
2	Y	$\pm 60^{\circ}$	σ_2	Y	$\pm 60^{\circ}$	σ_2	U	0°	σ_1^+
3	Y	0°	σ_2	Y	0°	σ_2	U	$\pm 60^{\circ}$	σ_1^+
4	Y	0°	σ_2	Y	0°	σ_2	U	$\pm 60^{\circ}$	σ_1^+
5	Y	0°	σ_2	Y	0°	σ_2	U	$\pm 60^{\circ}$	σ_1^+
6	Y	0°	σ_2	Y	0°	σ_2	Y	$\pm 60^{\circ}$	σ_{12}
7	Y	0°	σ_2	Y	0°	σ_2	Y	$\pm 60^{\circ}$	σ_{12}
8	U	0°	σ_1^-	Y	0°	σ_2	Y	$\pm 60^{\circ}$	σ_{12}
9	U	0°	σ_1^-	Y	$\pm 60^{\circ}$	$\sigma_2^{(5)}$	Y	$\pm 60^{\circ}$	σ_{12}
10	U	0°	σ_1^-	Y	$\pm 60^{\circ}$	σ_2	Y	$\pm 60^{\circ}$	σ_{12}

(1) Failure in Yield or Ultimate.
(2) Layer in Which Failure Occured.
(3) Stress Which Initiated Failure, 1 is in Fiber Direction (-Compression, + Tension).
(4) $N_y/N_x = \text{Tan}(m\pi/10.)$.
(5) Failure by Yielding in $\pm 60^{\circ}$ Layer, Caused by Shear Stress, Occurs Between These Two Points (8 and 9).

TABLE IX

FINAL WEIGHTS FOR 101 CONFIGURATION

SECTION	Weight, Lb. (Isotropic Laminate Except Where Noted).								
	Glass/Epoxy			Boron/Epoxy			Carbon/Aluminum		
	Monocoque	.005 Sand.	.001 Sand.	Monocoque	.005 Sand.	.001 Sand.	Monocoque	.005 Sand.	.001 Sand.
Instrument Unit	22554	7959	3640	13328	4718	1951	10882	3544	1455
Forward Skirt	33868	12008	5660	19984	7107	2945	16215	5333	2211
LH_2 Tank Top Head	6327	6327	6327	5951	5951	5951	6417	6417	6417
LH_2 Tank Cylinder	36138	43940	43205	18651	15970	15185	15207	13467	12917
LH_2 Tank Bottom Head	7508	7508	7508	7045	7045	7045	7620	7620	7620
Intertank	89210	32171	17315[a]	52357	18933	8011	42352	14159	6485[c]
Baffles & Insulation	23740	23740	23740	23740	23740	23740	23740	23740	23740
LOX Tank & Thrust Structure	54546	54546	54546	54546	54546	54546	54546	54546	54546
Aft. Skirt	241338	94461	56405	140361	52126	26251	112905	39172	21993[c]
2nd Stage Total	515229	282660	218346	335963	190136	145625	289824	167998	137384
Interstage	61591	23992	14271[a]	35836	13296	6643	28833	9984	5557[c]
Forward Skirt	105207	40322	23645[a]	61282	22658	11014	49343	16872	9166[c]
LOX Tank Top Head	5306	5306	5306	5026	5026	5026	5374	5374	5374
LOX Tank Cylinder	48746	21190	16612	28516	10613	6509	23023	8783	6491
LOX Tank Bottom Head	11408	11408	11408	10692	10692	10692	11582	11582	11582
Intertank	256604	101955	61548[a]	149098	55522	28631	119857	41852	24081[c]
RP-1 Tank Top Head	3057	3057	3057	2828	2828	2828	3110	3110	3110
RP-1 Tank Bottom Head	5614	5614	5614	5197	5197	5197	5716	5716	5716
Thrust Takeout	89954	36115	21951[a]	52235	19486	10208	41974	14729	8607[c]
Thrust Structure	81537	81537	81537	81537	81537	81537	81537	81537	81537
Baffles & Insulation	39270	39270	39270	39270	39270	39270	39270	39270	39270
1st Stage Total	708294	369766	284219	471517	266125	207555	409619	238809	200491
Total Weight	1223523	652426	502565	807480	456261	353180	699443	406807	337875
% Weight Savings	-61.8	+13.7	+33.5	-6.8	+39.7	+53.3	+7.5	+46.2	+55.3

a - Configuration (0^o-85% Thickness 90^o-15% Thickness)

b - Configuration (0^o-95% Thickness 90^o-5% Thickness)

c - Configuration (0^o-90% Thickness 90^o-10% Thickness)

TABLE X

FINAL WEIGHTS FOR 201 CONFIGURATION

SECTION	Weight, Lb. (Isotropic Laminate Except Where Noted)								
	Glass/Epoxy			Boron/Epoxy			Carbon/Aluminum		
	Monocoque	.005 Sand.	.001 Sand.	Monocoque	.005 Sand.	.001 Sand.	Monocoque	.005 Sand.	.001 Sand.
IU & Forward Skirt	31781	11248	5242	18763	6661	2759	15288	5001	2065
LH_2 Tank & Thrust Structure	39323	39323	39323	39323	39323	39323	39323	39323	39323
Intertank	98911	35249	17441	58248	20844	8663	47210	15622	6624
Baffles & Insulation	12900	12900	12900	12900	12900	12900	12900	12900	12900
LOX Tank	8850	8850	8850	8850	8850	8850	8850	8850	8850
Aft. Skirt	22802	8264	4539[a]	13360	4855	2122	10796	3628	1714[c]
2nd Stage Total	214567	115879	88295	151444	93433	74617	134307	85324	71476
Interstage	152415	55317	30586[a]	89259	32486	14294	72111	24264	11579[c]
Forward Skirt	108239	39798	21944[a]	63352	23097	10251	51163	17245	8331[c]
LOX Tank Top Head	9300	9300	9300	8739	8739	8739	9436	9436	9436
LOX Tank Bottom Head	12852	12852	12852	12044	12044	12044	13045	13045	13045
Intertank	304850	117593	69371[a]	177483	65717	32303	142860	49305	26944[c]
LH_2 Tank Top Head	6512	6512	6512	6157	6157	6157	6596	6596	6596
LH_2 Tank Cylinder	151502	88354	78765	88698	38019	29236	71645	30020	23915
LH_2 Tank Bottom Head	17848	17848	17848	16520	16520	16520	18169	18169	18169
Thrust Takeout	109199	42011	24724	63588	23531	11514	51190	17653	9595[c]
Thrust Structure	82741	82741	82741	82741	82741	82741	82741	82741	82741
Baffles & Insulation	20040	20040	20040	20040	20040	20040	20040	20040	20040
1st Stage Total	975498	492366	374683	628621	329091	243839	538996	288514	230391
Total Weight	1190065	608245	462978	780065	422524	318456	673303	373838	301867
% Weight Savings	-72.2	+12.0	+33.0	-12.9	+38.8	+53.9	+2.5	+45.9	+56.3

a - Configuration (0^o-85% Thickness 90^o-15% Thickness)

b - Configuration (0^o-95% Thickness 90^o-5% Thickness)

c - Configuration (0^o-90% Thickness 90^o-10% Thickness)

TABLE XI

FINAL WEIGHTS FOR 301 CONFIGURATION

SECTION	Weight, Lb. (Isotropic Laminate Except where Noted).								
	Glass/Epoxy			Boron/Epoxy			Carbon/Aluminum		
	Monocoque	.005 Sand.	.001 Sand.	Monocoque	.005 Sand.	.001 Sand.	Monocoque	.005 Sand.	.001 Sand.
Instrument Unit	35445	12627	6161	20884	7461	3100	16931	5594	2356
Forward Skirt	124788	44186	20648	73663	26163	10837	59781	19640	8116
LOX Tank Top Head	10561	10561	10561	10000	10000	10000	10697	10697	10697
LOX Tank Cylinder	12807	8074	7366	7609	3416	2768	6194	2731	2269
Common Bulkhead	32947	32947	32947	31659	31659	31659	33260	33260	33260
LH_2 Tank Cylinder	766295	314353	233719	447701	165951	96442	361163	137779	101517
LH_2 Tank Bottom Head	16024	16024	16024	15057	15057	15057	16258	16258	16258
Thrust Takeout	160689	62862	37521[a]	93460	34705	17463	75180	26078	14628[c]
Thrust Structure	56175	56175	56175	56175	56175	56175	56175	56175	56175
Insulation	18000	18000	18000	18000	18000	18000	18000	18000	18000
Total Weight	1233731	575809	439122	774208	368587	261501	653639	326212	263276
% Weight Savings	-92.4	+10.2	+31.5	-20.7	+42.5	+59.2	-1.9	+49.1	+58.9

a - Configuration
(0°-85% Thickness
90°-15% Thickness)

b - Configuration
(0°-95% Thickness
90°-5% Thickness)

c - Configuration
(0°-90% Thickness
90°-10% Thickness)

VEHICLE DATA

Gross Weight at Liftoff	20,139,000 lbs (9,135,050 Kg)
First Stage Thrust	
At Liftoff	25,200,000 lbs (112,089,600 N)
Nominal (Vacuum)	28,337,000 lbs (126,042,976 N)
Vehicle Reference Diameter	65.5 ft. (19.96 m)
Aerodynamic Reference Area	3,369.55 sq. ft. (313.03 sq. m)
Vehicle Length	415.4 ft. (126.61 m)
First Stage Effective Nozzle Exit Area	215,909 sq. in. (139.26 sq. m)
First Stage Propellant Weight Flow Rate	95,093 lb/sec (43.134 Kg/sec)
Propellant Mixture Ratio	
First Stage N-1 (LOX/RP-1)	2.25
Second Stage N-11 (LOX/LH_2)	5.0
Number of Engines	14 F-1/3 M-1
Nominal Vehicle Structural Weight	
Second Stage Structure	304,134 lbs (137,955 Kg)
First Stage Structure	452,171 lbs (205,105 Kg)
Total Vehicle Structure	756,305 lbs (343,060 Kg)
Nominal Payload	811,000 lbs (367,870 Kg)

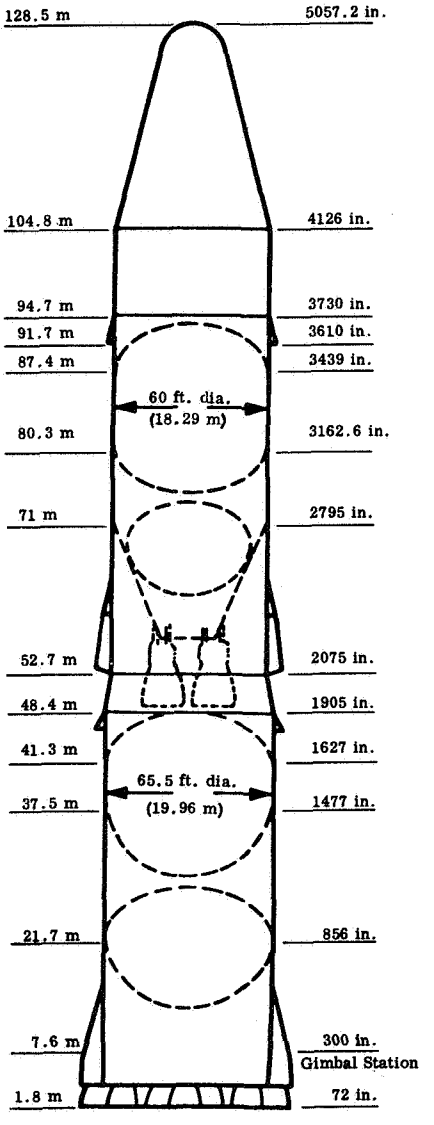

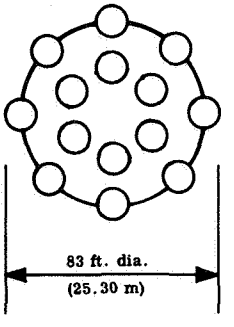

Figure 1. Vehicle 101 Configuration
(Ref. 2, Vol. 2)

VEHICLE DATA

Gross Weight at Liftoff	14,400,000 lbs (6,531,840 Kg)
Thrust	
At Liftoff	18,000,000 lbs (80,064,000 N)
Nominal (Vacuum)	21,851,000 lbs (97,193,248 N)
Vehicle Reference Diameter	70 ft. (21.34 m)
Aerodynamic Reference Area	3,848.45 sq. ft. (357.52 sq. m)
Vehicle Length	422.5 ft. (128.78 m)
Effective Nozzle Exit Area	262,044 sq. in. (169.02 sq. m)
Propellant Weight Flow Rate	47,452 lb/sec (21,524 Kg/sec)
Propellant Mixture Ratio	
N-1 (LOX/LH_2)	6.5
N-11 (LOX/LH_2)	6.5
Number of Engines	18/2 High Pressure
Nominal Vehicle Structural Weight	
Second Stage Structure	123,429 lbs (55,987 Kg)
First Stage Structure	567,393 lbs (257,369 Kg)
Total Vehicle Structure	690,822 lbs (313,356 Kg)
Nominal Payload	1,019,000 lbs (462,218 Kg)

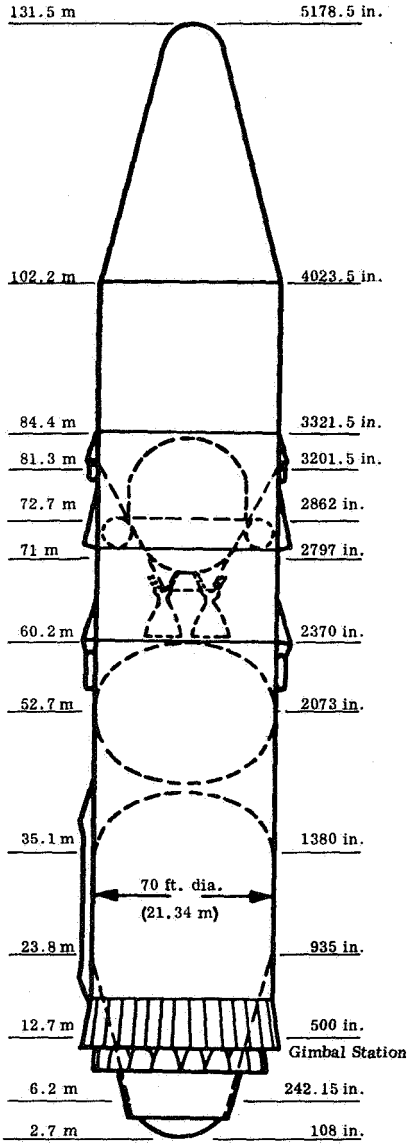

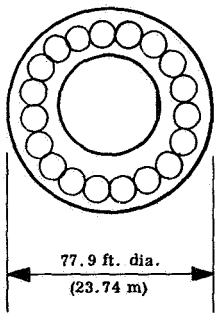

Figure 2.. Vehicle 201 Configuration
(Ref. 2, Vol. 2)

VEHICLE DATA

Gross Weight at Liftoff	24,000,000 lbs (10,886,400 Kg)
Thrust	
At Liftoff	30,000,000 lbs (133,440,000 N)
Nominal (Vacuum)	35,570,000 lbs (158,215,360 N)
Vehicle Reference Diameter	80.0 ft. (24.38 m)
Aerodynamic Reference Area	5,026.548 sq. ft. (466.966 sq. m)
Vehicle Length	402.1 ft. (122.57 m)
Effective Nozzle Exit Area	379,008 sq. in. (244.46 sq. m)
Propellant Weight Flow Rate	79,576 lb/sec (36,096 Kg/sec)
Propellant Mixture Ratio	(LOX/LH_2) 7.0
Number of Engine Modules	24 High Pressure
Nominal Vehicle Structural Weight	641,320 lbs (290,903 Kg)
Nominal Payload	1,358,000 lbs (615,989 Kg)

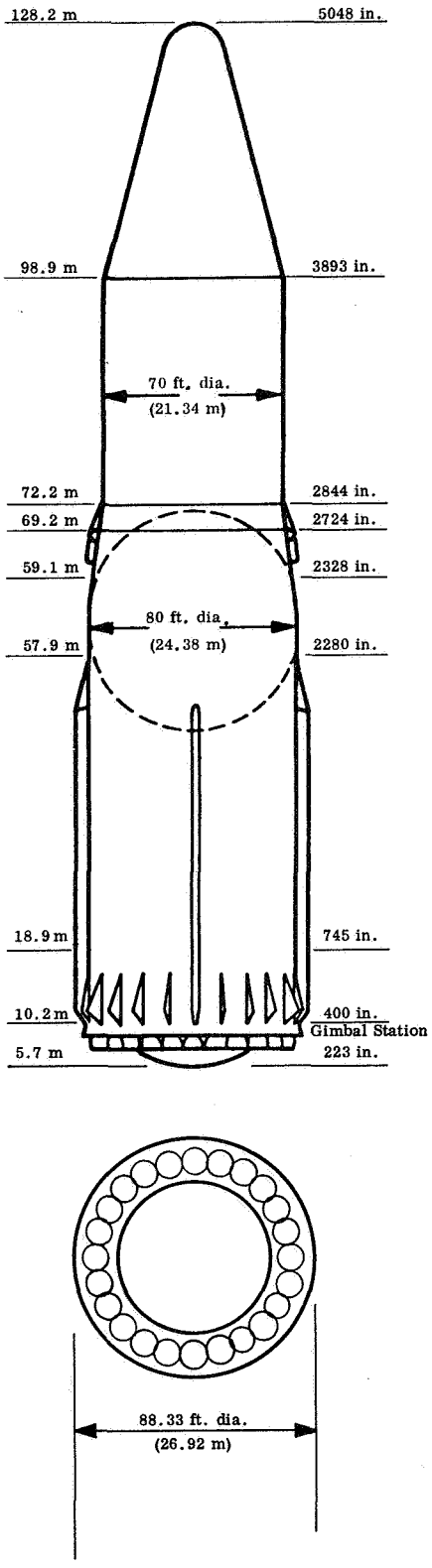

Figure 3. Vehicle 301 Configuration
(Ref. 2, Vol. 2)

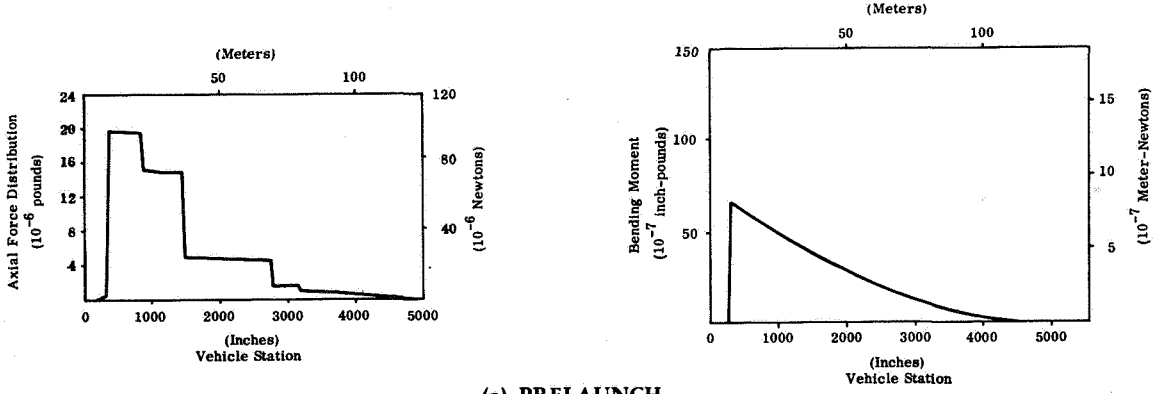

(a) PRELAUNCH

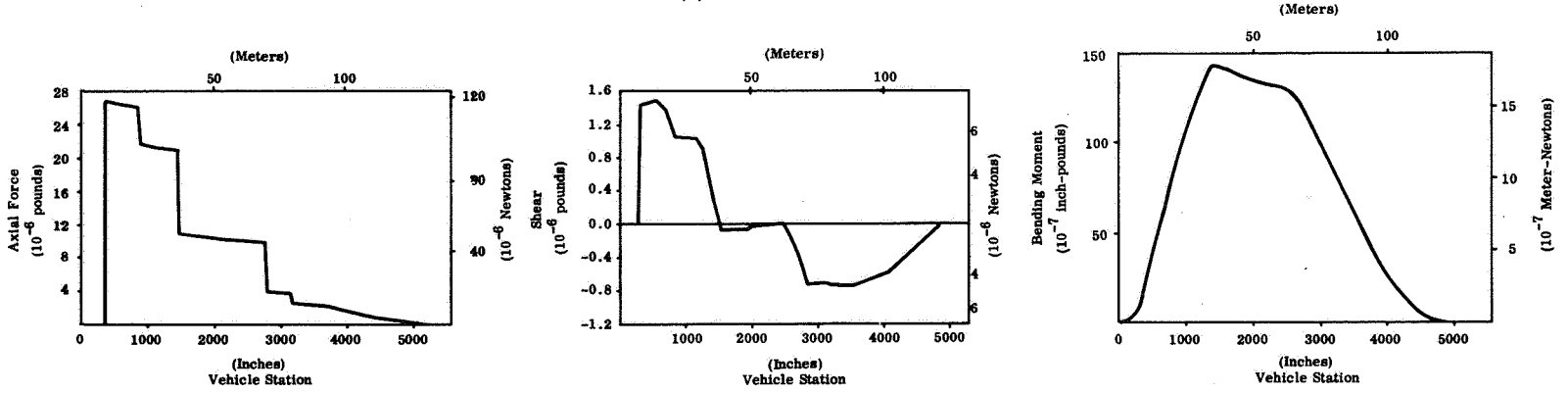

(b) MAXIMUM qα

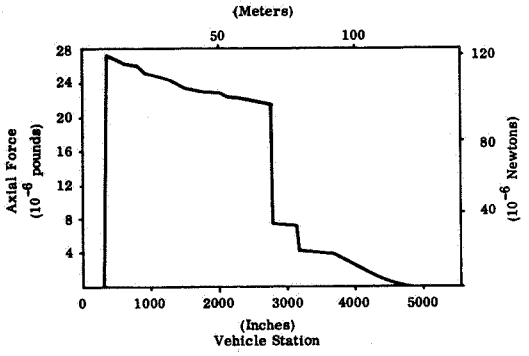

(c) MAXIMUM ACCELERATION

Figure 4. Nominal Load Distributions For the 101 Vehicle Configuration (Ref. 2, Vol. 2)

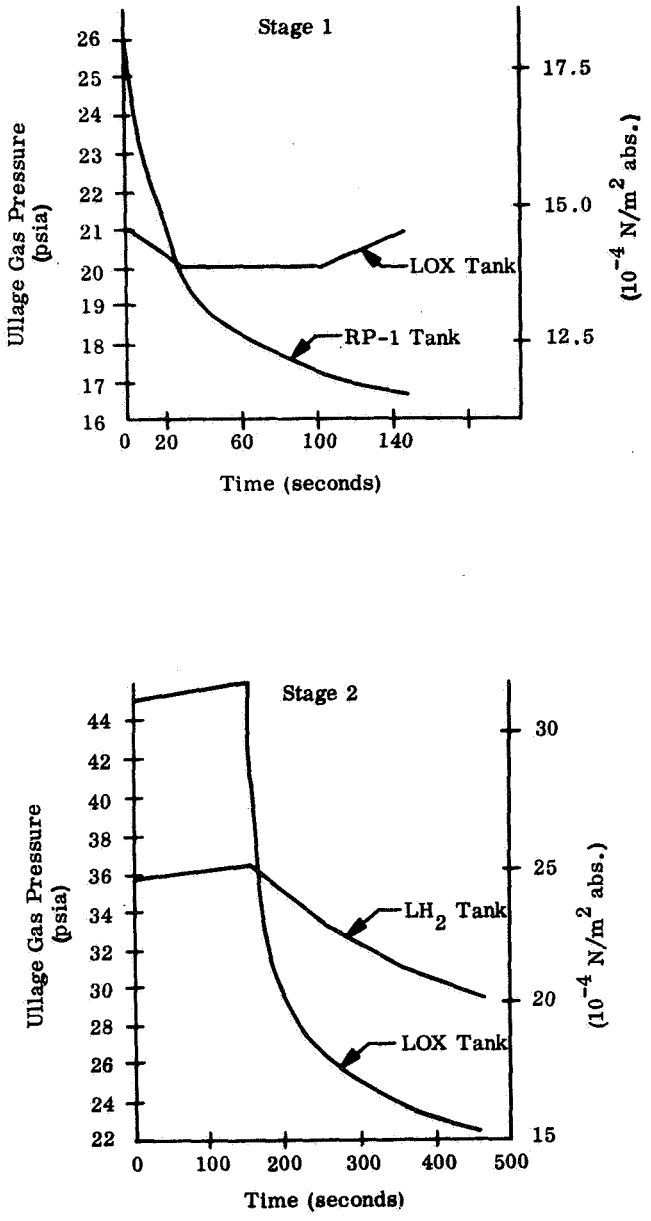

Figure 5. Propellant Tank Pressure Profiles for the 101 Vehicle Configuration

(Ref. 2, Vol. 2)

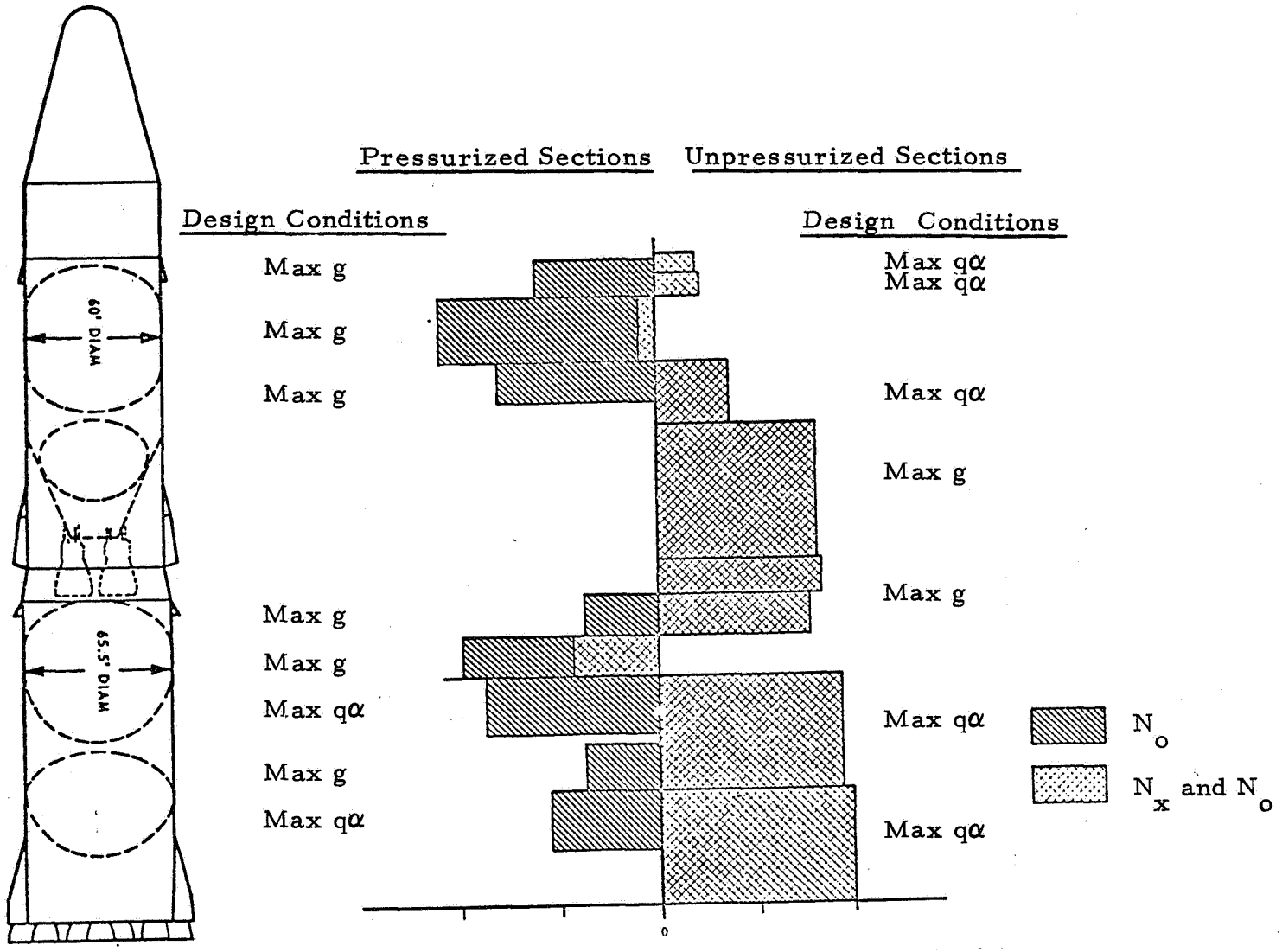

Figure 6. Envelope of Minimum Uniaxial Load, N_x, and Effective Uniaxial Load for Combined Stress, N_o, for the 101 Configuration.

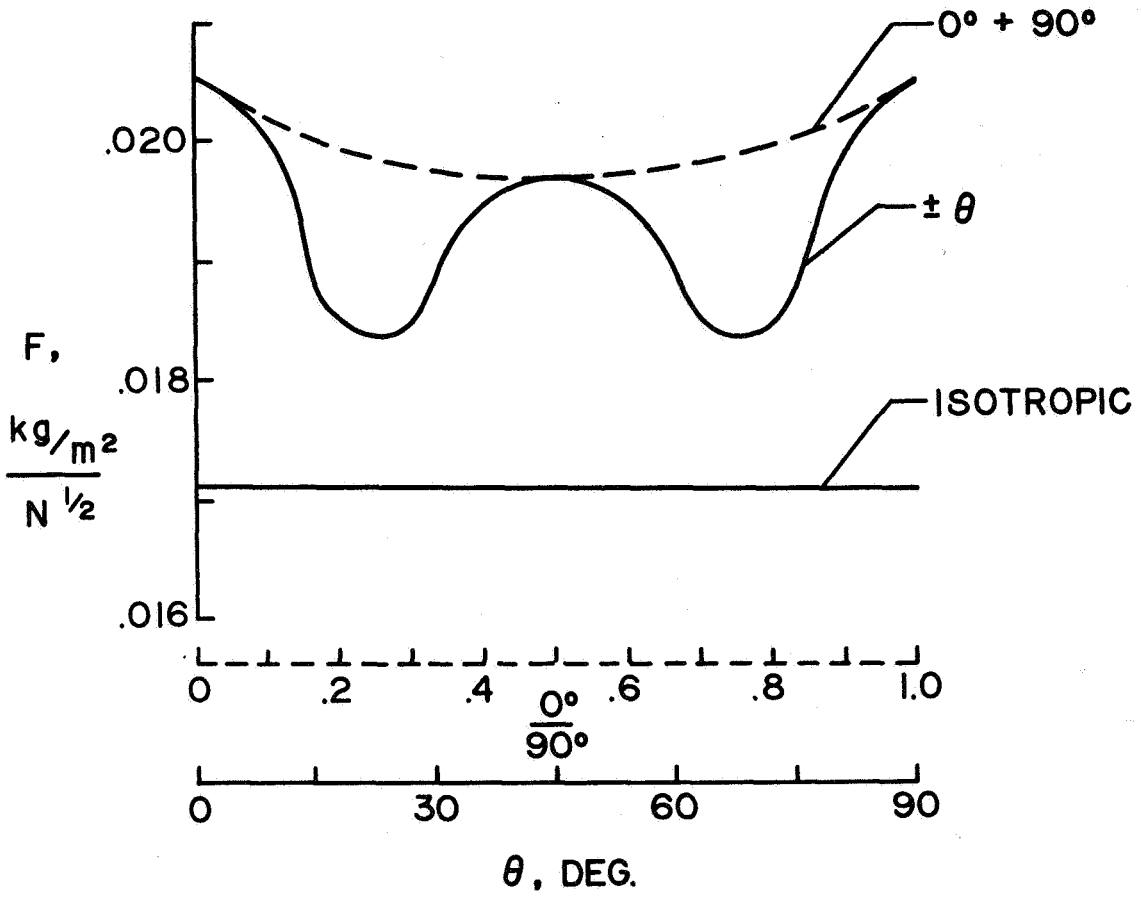

Figure 7. Variation of Elastic Structural Efficiency of Biaxial Laminates of E-Glass Fibers in an Epoxy Matrix. (Ref. 8)

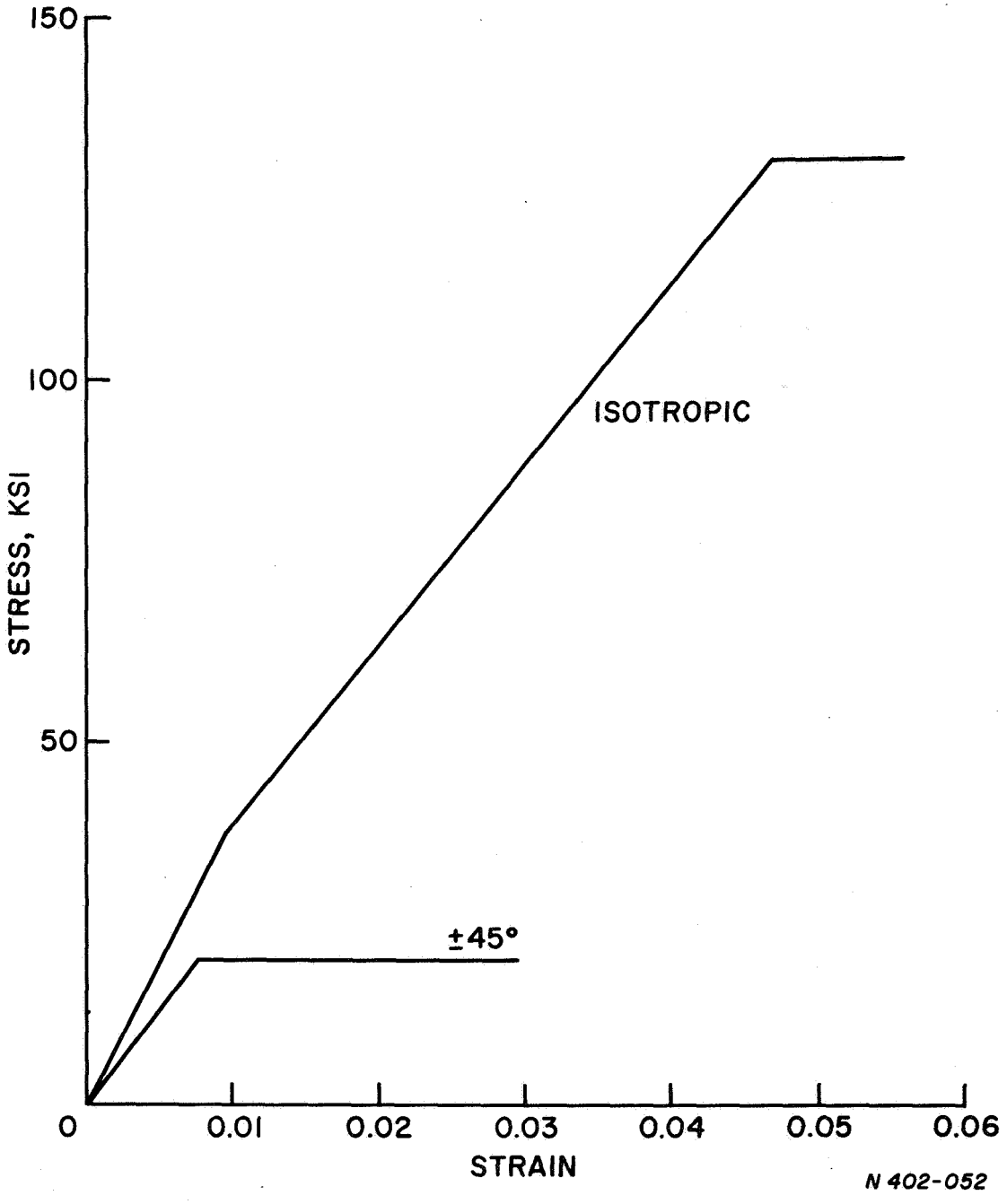

Figure 8. Calculated Stress-strain Curves for E-Glass and Epoxy Composite Laminates. (Ref. 11)

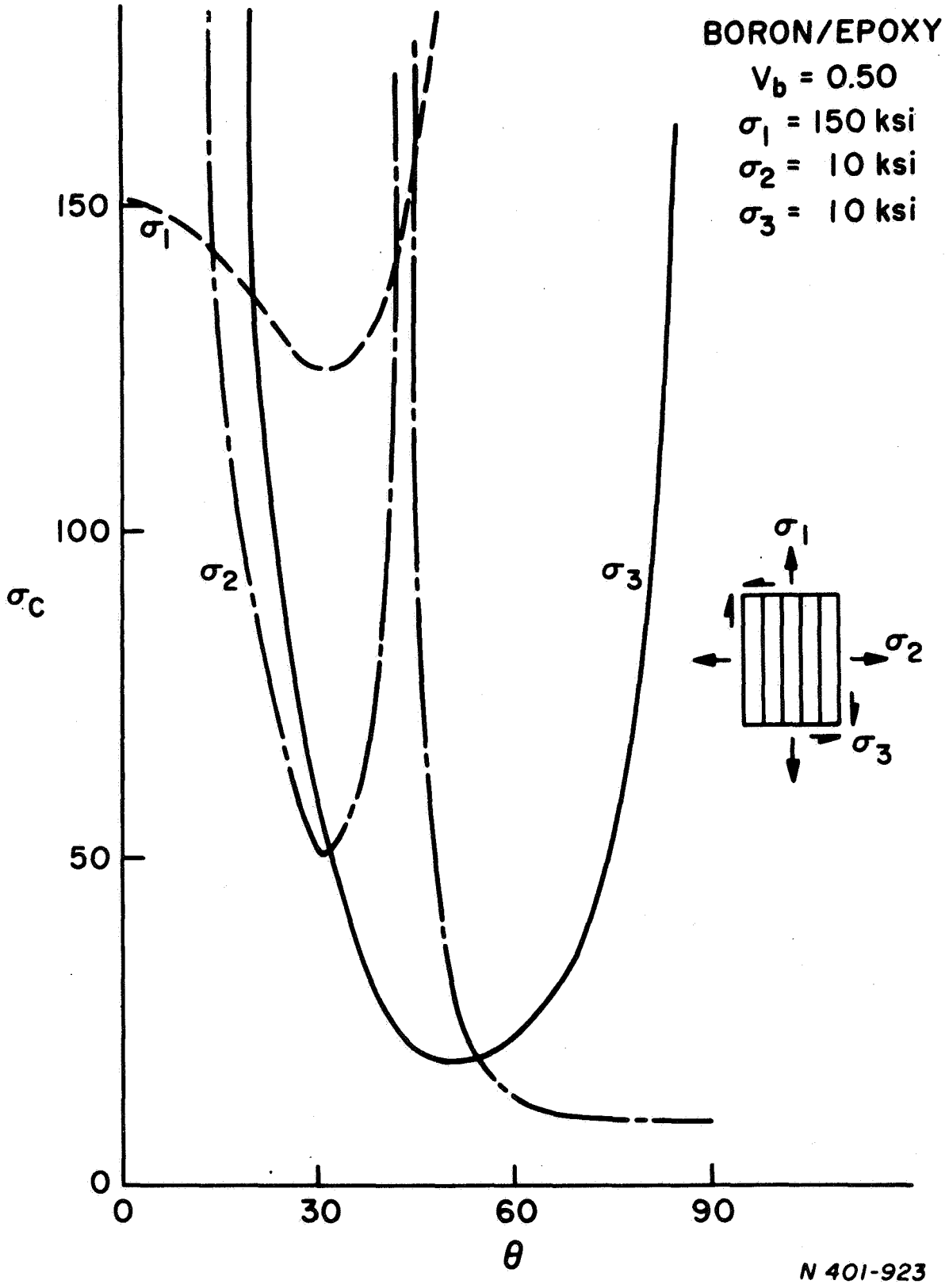

Figure 9. Yield Strength of a Symmetric Bi-axial Composite Laminate for Failure Modes Involving Each of the Principal Lamina Stresses. (Ref. 11)

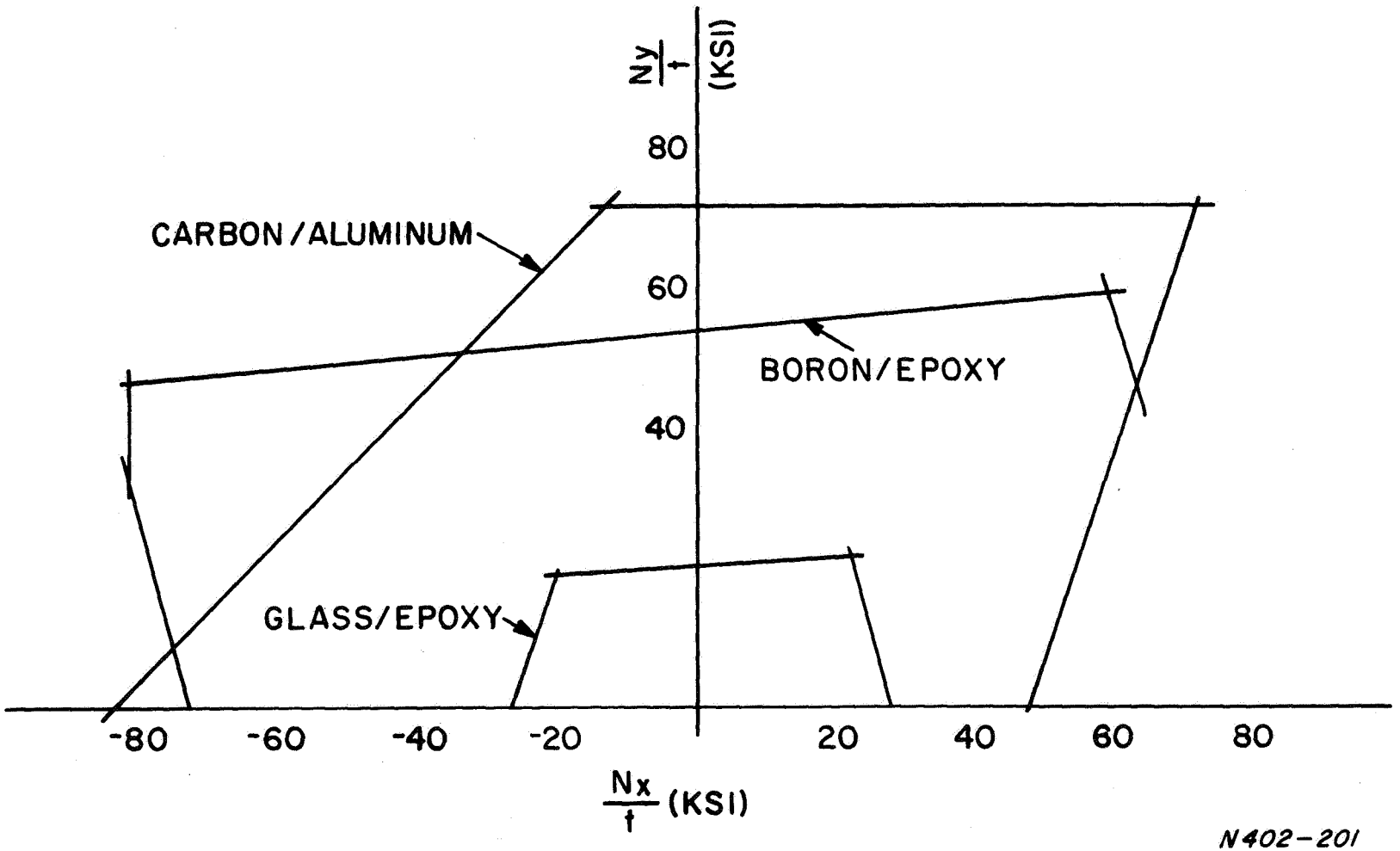

Figure 10. Interaction Curves Isotropic Laminate

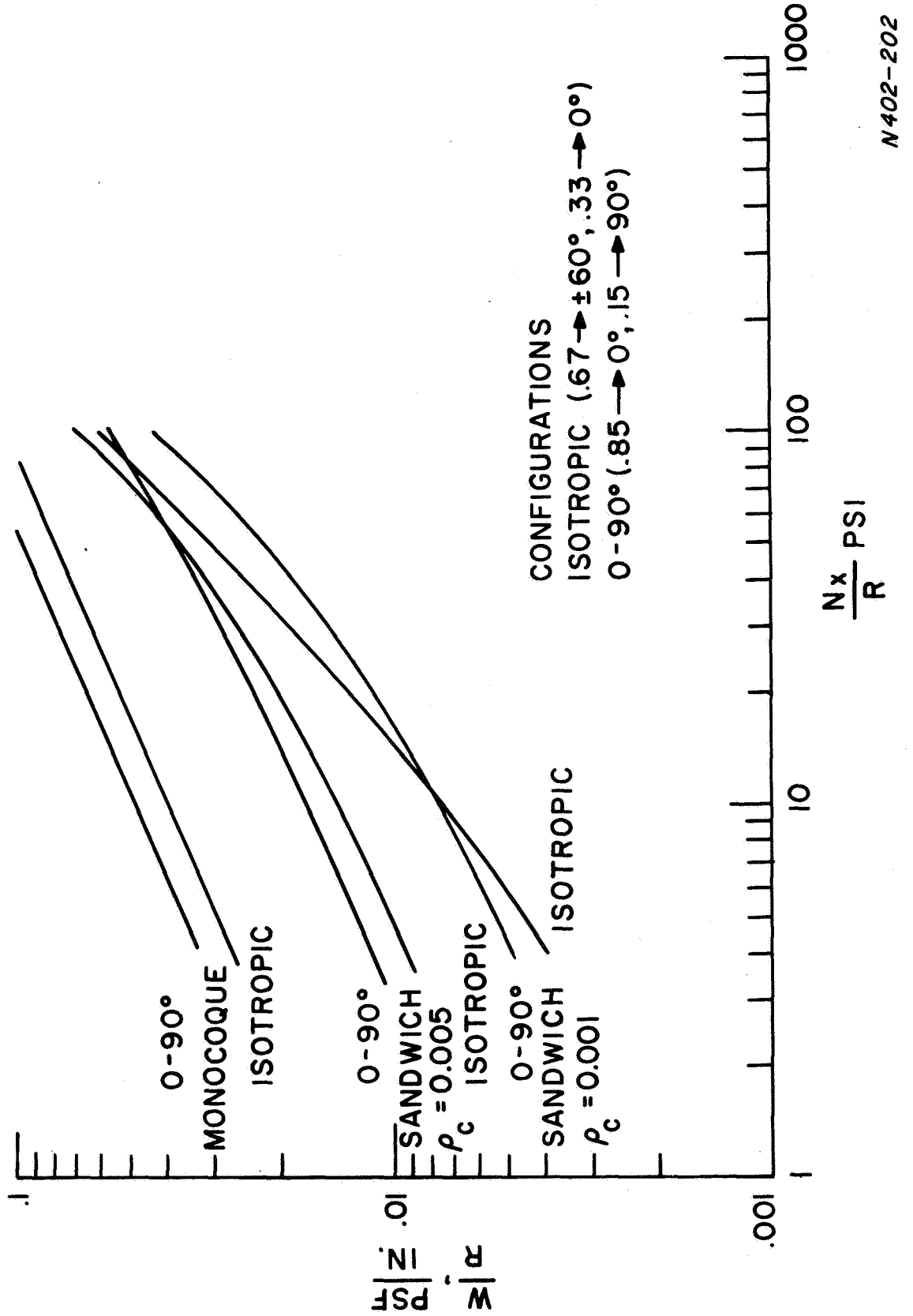

Figure 11. Glass/Epoxy Efficiency Curves Axial Compression

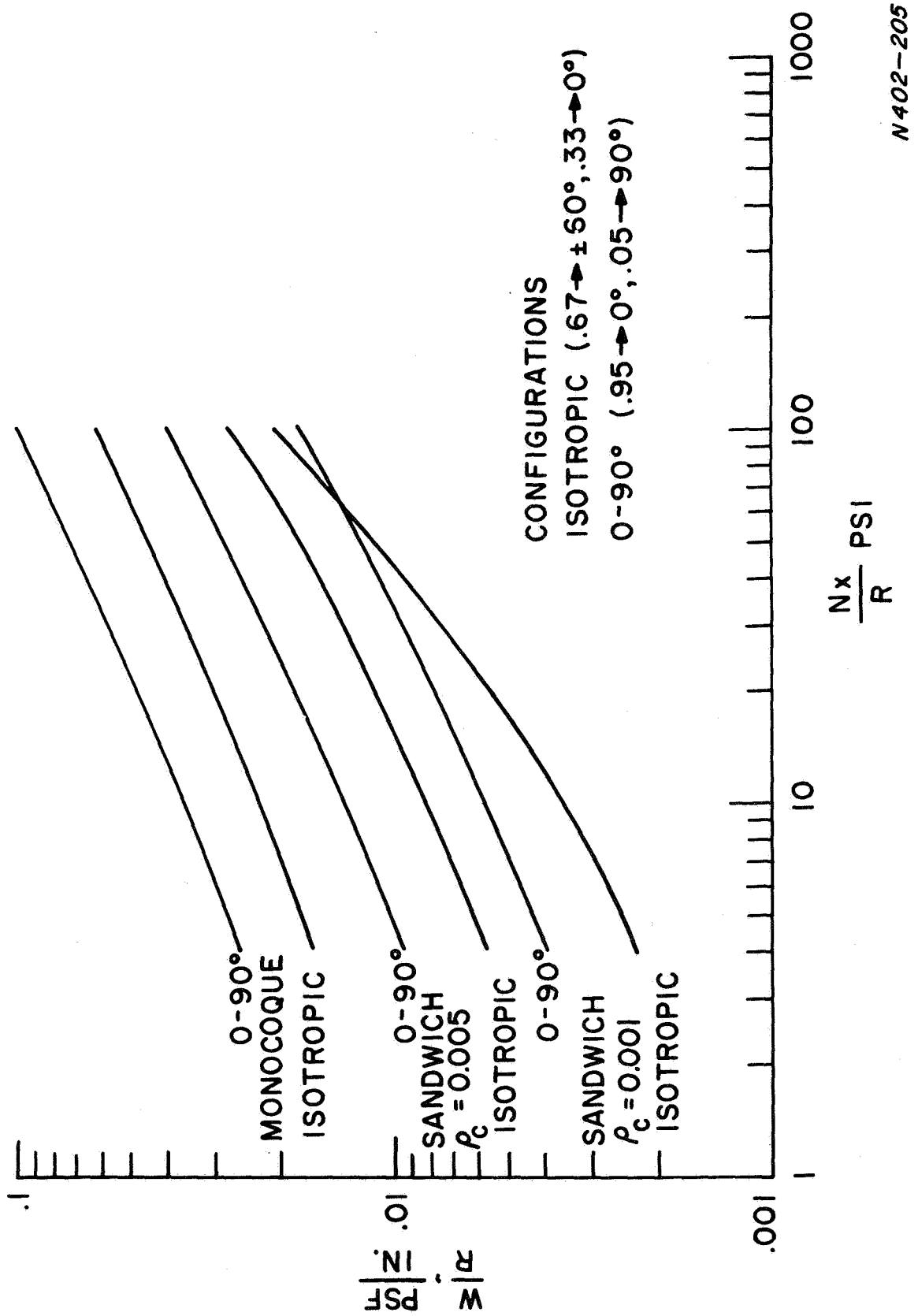

Figure 12. Boron/Epoxy Efficiency Curves Axial Compression

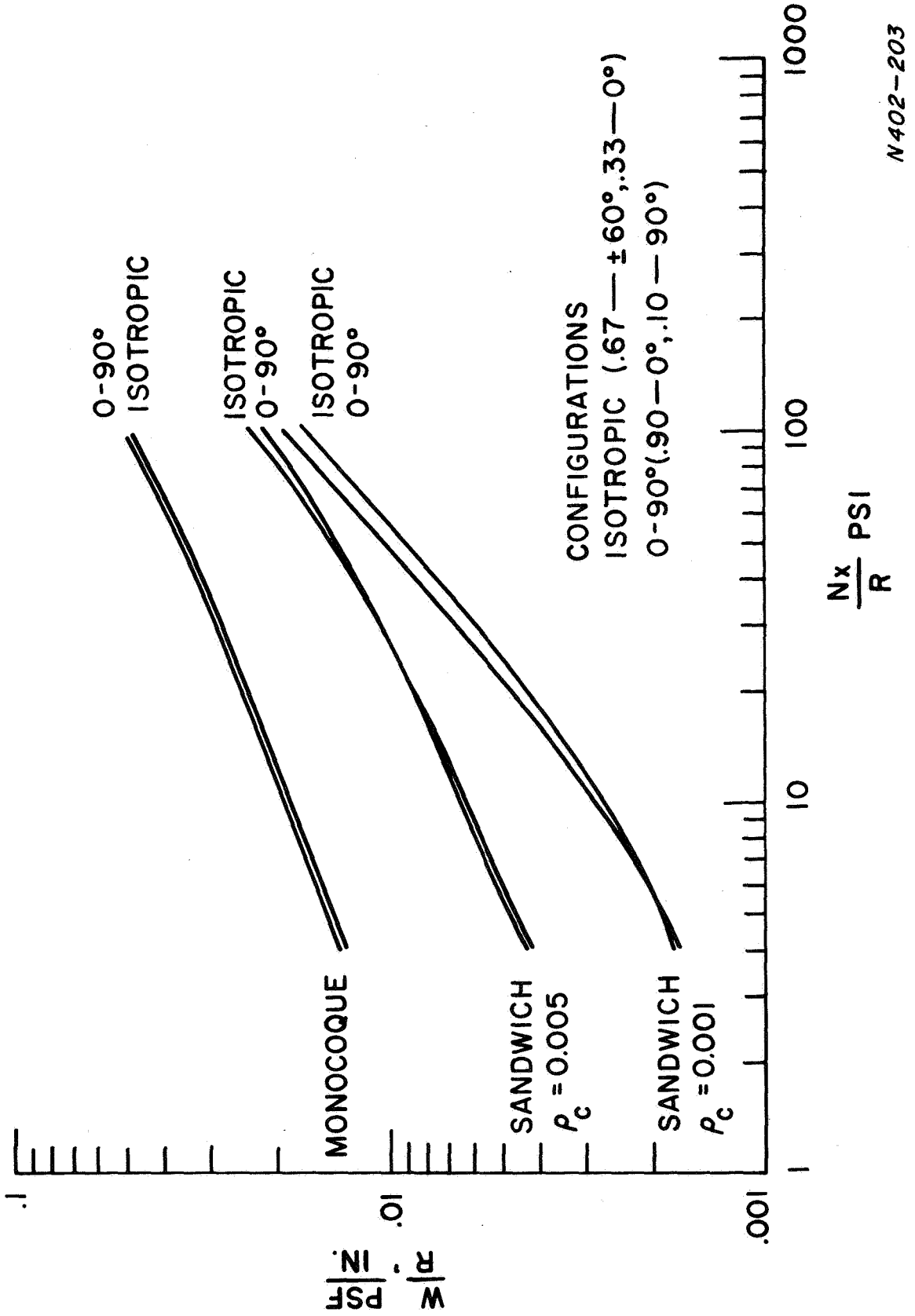

Figure 13. Carbon/Aluminum Efficiency Curves Axial Compression

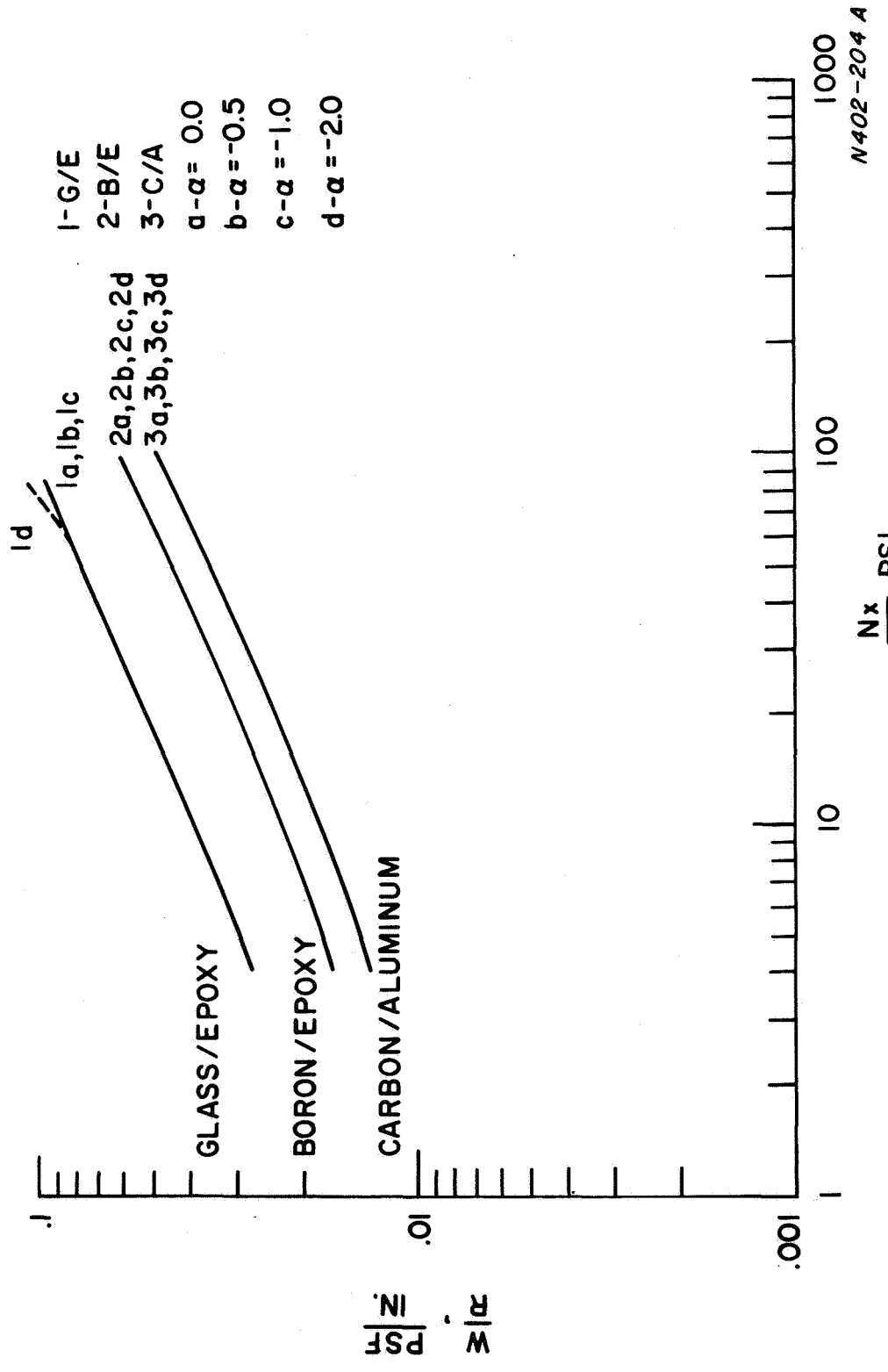

Figure 14. Isotropic Laminate Monocoque Shell $\alpha = N_y/N_x$

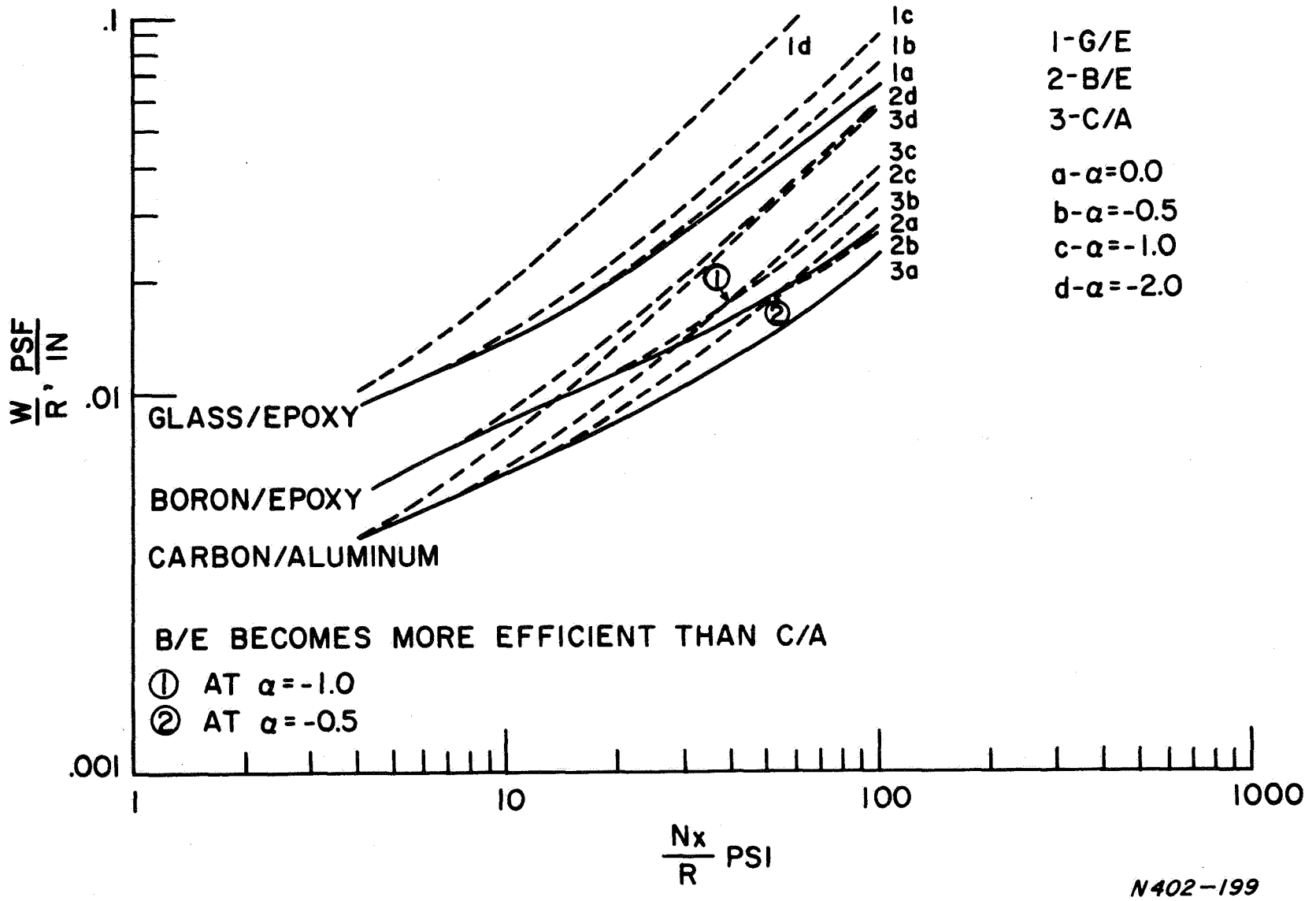

Figure 15. Isotropic Laminate Sandwich Shell ($\rho_c = 0.005$) $\alpha = N_y/N_x$

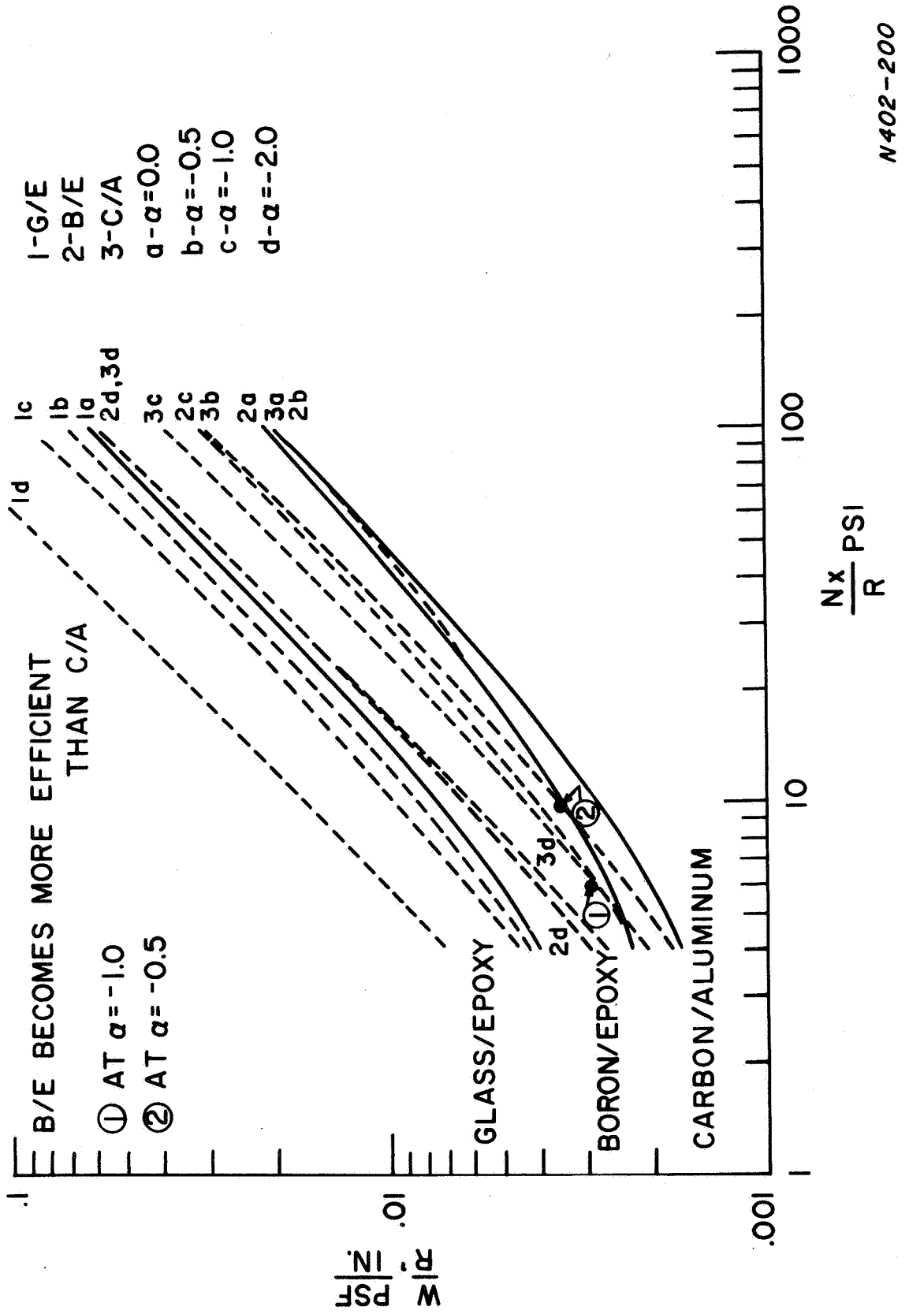

Figure 16. Isotropic Laminate Sandwich Shell ($\rho_c = 0.001$) $\alpha = N_y/N_x$

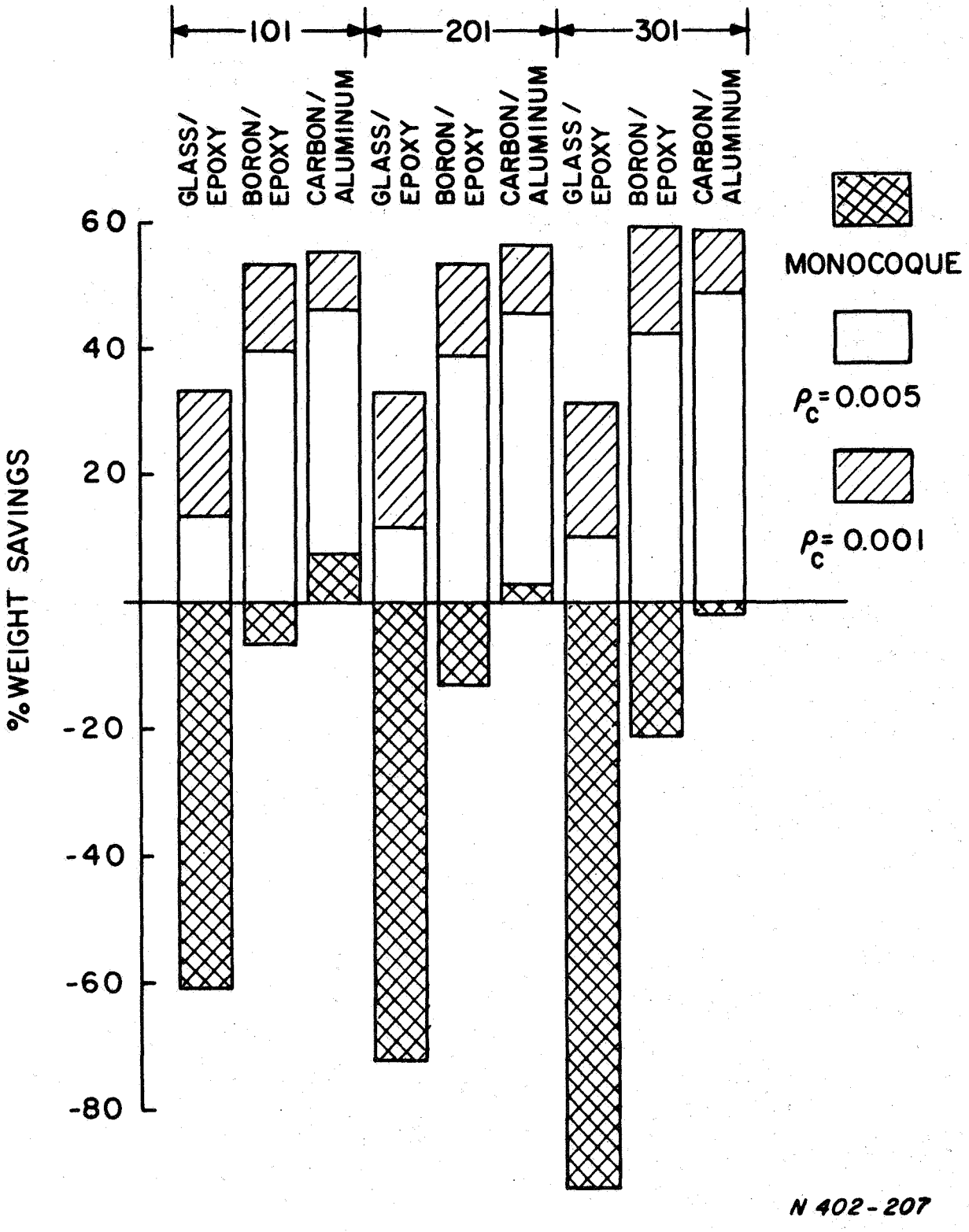

Figure 17. Percent Weight Savings for Three Configurations

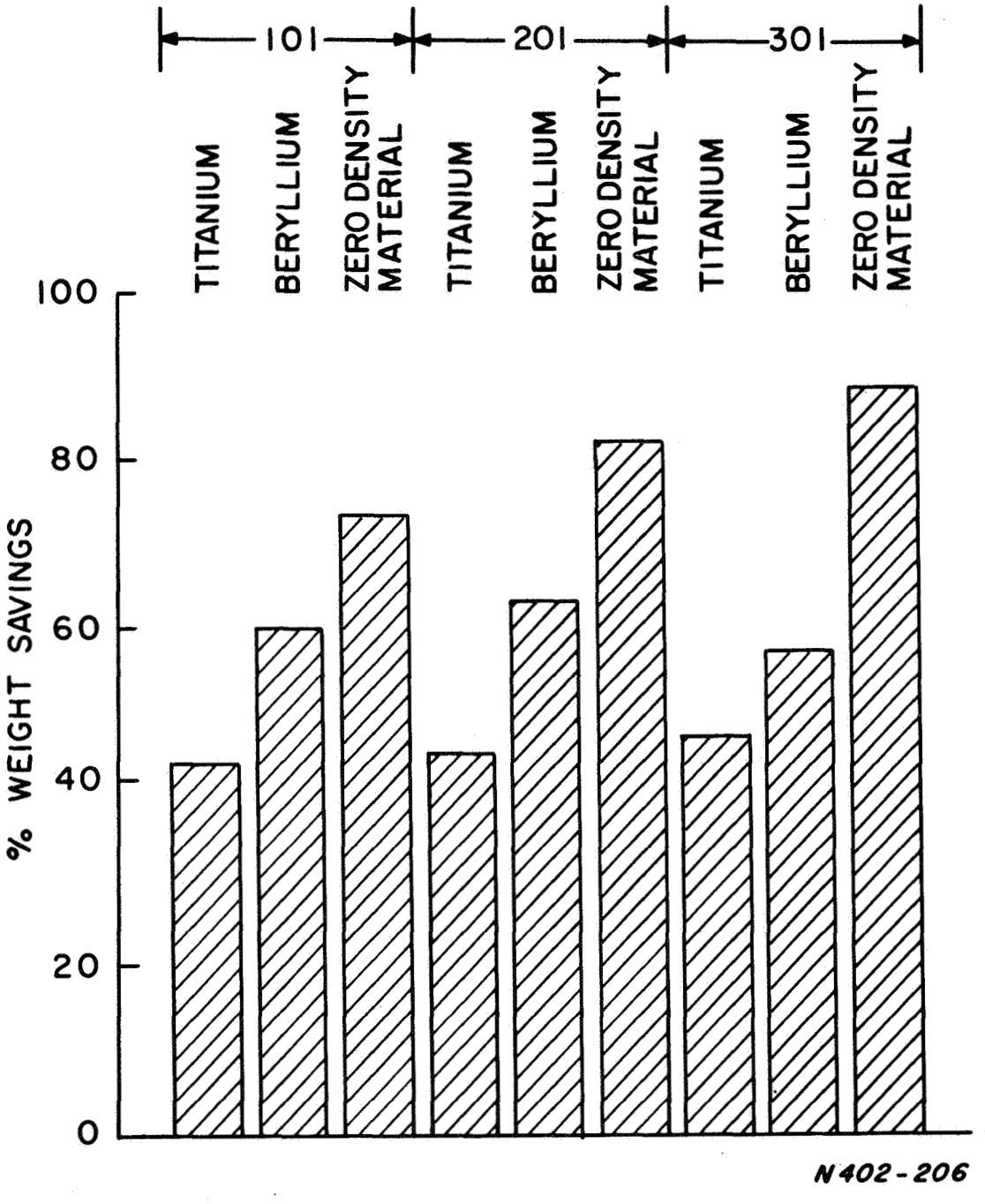

Figure 18. Percent Weight Savings (For Comparison with Figure 17). From Ref. 2.

GENERAL ELECTRIC

SPACE SCIENCES LABORATORY
MISSILE AND SPACE DIVISION

TECHNICAL INFORMATION SERIES

AUTHOR	SUBJECT CLASSIFICATION	NO.
B. W. Rosen, et al.	Composite Materials	R67SD57
		DATE: Oct. 1967
TITLE: APPLICATION OF FIBROUS COMPOSITE MATERIALS TO LARGE ROCKET SYSTEMS		G. E. CLASS: I
		GOV. CLASS: Unc.
REPRODUCIBLE COPY FILED AT MSD LIBRARY, DOCUMENTS LIBRARY UNIT, VALLEY FORGE SPACE TECHNOLOGY CENTER, KING OF PRUSSIA, PA.		NO. PAGES: 52

SUMMARY

Studies of the potential for minimization of structural weight in large launch vehicles of the future through the use of composite materials are described. Previous structural weight minimization techniques for composites are reviewed and extended. Typical structural efficiency charts are presented. Significant weight savings through the application of an efficiently stiffened composite structure is demonstrated.

KEY WORDS: Fibrous composites, efficiency, aerosapce structures.

BY CUTTING OUT THIS RECTANGLE AND FOLDING ON THE CENTER LINE, THE ABOVE INFORMATION CAN BE FITTED INTO A STANDARD CARD FILE.

AUTHOR B. W. Rosen

COUNTERSIGNED F. N. Hauth